Manuscript # acp-2017-455

Reply to Referee #1

We are very grateful to all important and helpful comments from the referee. The followings are our responses to each comment in detail.

5

This study quantifies the relationship among $PM_{2.5}$ concentration, visibility and planetary boundary layer height for long–lasting haze and fog–haze mixed events in Beijing city. They found negative relationships between visibility and $PM_{2.5}$, $PM_{2.5}$ and PBL height. They also found a double inversion layer formed in both typical events, which played critical roles in maintaining and enhancing the long–lasting polluted events. The topic of this paper is interesting and is suitable for publication in this journal. However, some improvements are needed before publication. Following are the major and specific issues:

Major issues:

1. The authors provided a large amount information of the relationships between $PM_{2.5}$, visibility and PBL height. However, these relationships are reported in many previous studies. The new finding in this study about influence double inversion layer on the meteorology and $PM_{2.5}$ needs more attention and discussion.

15 **Reply 1:**

Thanks for your constructive suggestions. We added some discussions relevant to our new finding about influence of double inversion layer on the polluted events in the conclusions and discussions section, as "The new finding in this paper has important implications in explaining the frequent long–lasting polluted events in the study region. Generally, a typical pollution event is usually formed under a stable and shallow temperature–inversion condition at low atmospheric layers, and would

20 disappear or obviously decrease when the daytime solar radiation increases. However, in the study region, we found that many severe haze and fog–haze mixed events lasted for several days even for several weeks. Most previous publications attributed the reason as the persistent abnormal weather system or high emissions. However, this study shows that except for the influence of meteorological condition and high emission, the interactions and feedbacks between PBL and aerosol loading linked by radiation process are crucial in enhancing and maintaining these polluted events. These feedbacks could cause an important

25 variation of dynamical/thermal processes in lower troposphere. The formation of double inversion layer and their subsequent change is closely associated with persistent meteorological condition, high aerosol loading and associated radiation process. Due to the complex interactions and feedbacks, a deeper and more stable atmospheric low–level inversion layer is formed and it is hard to break up by daytime solar radiation heating process until the strong wind occurs and removes the high aerosol loading."

30

Specific issues:

1

2. Abstract: Causal relationship about 'The air quality and visibility are strongly influenced by aerosol loading and meteorological conditions.' It would be better to revise as 'influenced by aerosol loading, which is driven by meteorological conditions'.

Reply 2:

Thanks for the suggestion. It has been corrected in the revised manuscript.

3. Introduction: Haze in China is a very hot topic and raises a bunch of new studies recently. The authors may cite more recent papers to strengthen this part. Climate change (Cai et al., 2017, Nature Climate), Arctic sea ice loss (Zou et al., 2017, Science Advances) and decadal weakening of winds (Yang et al., 2016, JGR) suggested causes in climate view. Dust-wind interaction (Yang et al., 2017a, Nature Communications) and upwind transport (Yang et al., 2017b, ACP) can also intensify haze in China.

Reply 3:

Thanks for the good suggestion. We have added some recent papers in the introduction section based on your suggestion, as "In addition, the interactions between aerosol pollution and climate change have been substantially addressed in recent publications, for example, anthropogenic climate change (Cai et al., 2017), reduced Arctic sea ice (Wang et al., 2015; Zou et al., 2017), the Tibetan Plateau warming (Xu et al., 2016), influences of ENSO events on haze frequency in eastern China (Gao and Li, 2015), weakened East Asian winter monsoon (Li et al., 2016), decadal weakening of winds (Yang et al., 2016), and enhanced thermal stability of the lower atmosphere (Zhang et al., 2014; Chen and Wang, 2015). The dust–wind interaction (Yang et al., 2017a) and upwind transport (Yang et al., 2017b) could also intensify haze events in China."

4. Page 6 Line 25: Why haze and fog-haze events were defined like this? The author mentioned humidity in the introduction but the fog-haze was not defined based on humidity.

Reply 4:

Thanks for the comment. Actually, the definition we used is from international definition of fog event. Fog is an observed horizontal visibility below 1000 m in the presence of suspended water droplets and/or ice crystals (NOAA, 1995), which means that when the horizontal visibility is below 1000 m, the fog events occur. Since the horizontal visibility for atmospheric haze event is usually larger than 1000 m, only the fog occurs the visibility can decrease to be less than 1000 m. So that is why we use the minimum visibility to define fog and haze events.

Theoretically, when a fog event occurs, the RH has to reach over 100 %. However, it is difficult to measure RH accurately, so in most cases, we use RH value of 90 % or 95 % as criterion to separate fog and haze. In fact, in the study region, when the RH is high enough, the fog and haze are usually co-existed. The haze aerosols can be transformed to fog droplets under certain conditions according to the Köhler curve (Köhler, 1936). It should be noticed that the situations such as heavy rain event or light fog events, which cause the horizontal visibility to be below or above 1000 m are not considered here. In addition, since we focus on long–lasting severe fog and haze event, we also include factors such as the lasting time and $PM_{2.5}$ mass concentration as additional criteria. To be more clearly, the corresponding text have been modified in the manuscript.

2

We also revised Table 1 to include more parameters such as duration and maximum RH of the pollutant events, show as below:

Table 1: The long–lasting haze and fog–haze mixed events from January 2014 to March 2015 in Beijing city

Type	Starting date / time	Ending date / time	Minimum visibility (m)	Duration (h)	Maximum PM$_{2.5}$ ($\mu g\ m^{-3}$)	Maximum RH (%)	Weather phenomenon
Haze events	2014.01.21/ 15:00	2014.01.24/ 15:00	1364	73	264	68	–
	2014.04.11/ 22:00	2014.04.14/ 23:00	1113	74	304	89	–
	2015.02.12/ 21:00	2015.02.16/ 10:00	1667	86	263	77	–
	2015.03.04/ 22:00	2015.03.08/ 10:00	1886	83	266	72	–
Fog–haze mixed events	2014.02.19/ 21:00	2014.02.26/ 20:00	647	168/76[b]	269	92	02.26/16:00–21:25 Drizzle rain
	2014.03.22/ 22:00	2014.03.28/ 14:00	664	137/13[b]	417	94	3.28/4:30–6:20 Drizzle rain
	2014.10.06/ 22:00	2014.10.11/ 18:00	500	117/48[b]	391	100	10.08/6:40–7:50 10.08/10:30–11:50 Drizzle rain
	2014.10.16/ 21:00	2014.10.20/ 23:00	964	99/3[b]	322	100	–
	2014.10.22/ 4:00	2014.10.26/ 4:00	258	97/24[b]	379	100	–
	2014.10.28/ 23:00	2014.11.01/ 5:00	837	79/1[b]	184	100	10.29/23:00– 10.30/00:10 10.31/15:10–16:30 Drizzle rain
	2015.01.12/ 17:00	2015.01.16/ 3:00	526	83/8[b]	297	93[a]	01.14/10:00–10:20 snow

[a] the maximum RH of all valid data except missing measurements.
5 [b] fog–haze mixed event duration / fog duration.

5. Figure 3: Are the both MPL and CL31 at site in Beijing?

Reply 5:

Yes, they are all located in the observational site at the campus of China Meteorological Administration (CMA) in Beijing. CL31 was sited on the roof of a 20 m tall building, and MPL installed in a working container beside the building not far away 10 m. To be more clearly, we have modified the corresponding text in section 2.1 as "The vertical profiles of aerosol in the troposphere and the PBL height could be also obtained from a ground–based MPL installed in a working container 10 m far away from the building at the campus of CMA."

6. Page 8 Line 21: How about these PBL height in haze events?

Reply 6:

Thank you for your questions. The $PM_{2.5}$ concentrations of 100 µg m^{-3}, 200 µg m^{-3}, 300 µg m^{-3} corresponded to the PBL heights of 460 m, 370 m and 280 m, respectively. It has been added in section 3.2 of the revised manuscript.

7. Page 9 Section 3.4.1: Why the authors chose April 2014 as the typical haze? Haze in northern China are more severe in winter season. How about the results for other haze events identified in this study?

Reply 7:

Thank you for your questions. As you said, the haze events in winter season in northern China are usually more severe. As seen in Table 1, there were only four long–lasting haze events during January 2014 to March 2015 in Beijing. The maximum $PM_{2.5}$ concentration was the highest and the corresponding data was relatively complete in the haze event in April 2014, so we choose the case as the type haze event. We have added these descriptions in section 3.4 of the revised manuscript. Our main conclusion about the influence of double inversion layer on the long–lasting pollution events in Beijing city are also suitable to the cases in Table 1.

8. Page 9 Line 25: The unit of visibility is m here but km in previous figures. Please unify units for the whole figures and manuscript.

Reply 8:

Thanks for the suggestion. The units of visibility and PBL height as 'm' for the whole figures and texts are unified in the revised manuscript, shown as below:
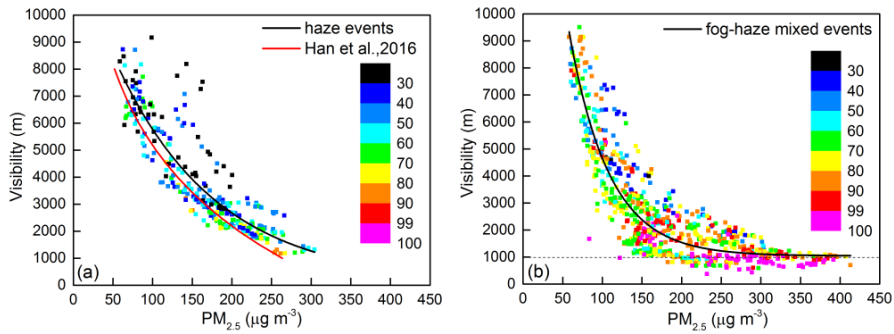
Figure 2: Relationship between the measured visibility and PM$_{2.5}$ mass concentration under different RH conditions for (a) haze and (b) fog–haze mixed events from January 2014 to March 2015 in Beijing city. The black exponential curves present the fits of the squares. The red exponential curve is the fit of daily averaged visibility and PM$_{2.5}$ concentration from October 2013 to September 2014 on stable meteorological days in Han et al. (2016)
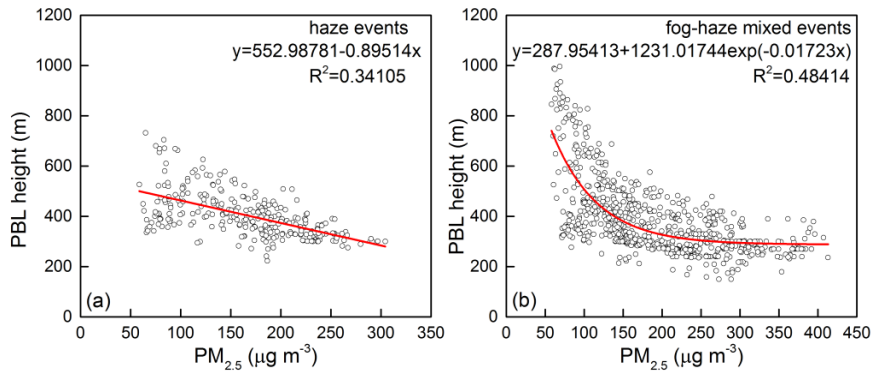

Figure 3: Relationship between PBL height and PM$_{2.5}$ mass concentration for (a) haze and (b) fog–haze mixed events from January 2014 to March 2015 in Beijing city
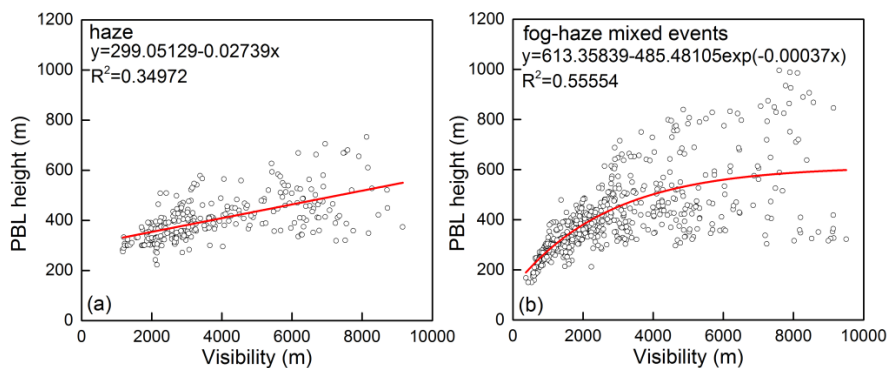
Figure 4: Relationship between visibility and PBL height for (a) haze and (b) fog-haze mixed events from January 2014 to March 2015 in Beijing city

9. Figure 6: I am confused that why PMcoarse did not increase with time. If aerosols are accumulated in the boundary layer due to decrease in PBL, all coarse and fine aerosol concentrations are expected to increase.

Reply 9:

Thanks for the comment. This is caused by the much lower value of PMcoarse than fine aerosol concentration. If we redraw the figures for the haze event and fog–haze mixed event (see below Fig. A and Fig. B), we can find almost the same tendency. The left vertical axis represents the concentration of $PM_{2.5}$ and PM_{10}. The right vertical axis represents the PMcoarse ($PM_{2.5–10}$) concentration. In general, the variation trend of PMcoarse is consistent with that of $PM_{2.5}$ in both two cases, especially in the fog–haze mixed event. In the previous manuscript, we used single vertical axis for the concentration of $PM_{2.5}$, PMcoarse and PM_{10} and the variation of PMcoarse concentration is not clear due to its lower value. Since the variation trend of PMcoarse was generally consistent with that of $PM_{2.5}$ in both two cases, so we have deleted the lines of PMcoarse in Fig. 5 (e) and Fig. 10 (e) in the revised manuscript.
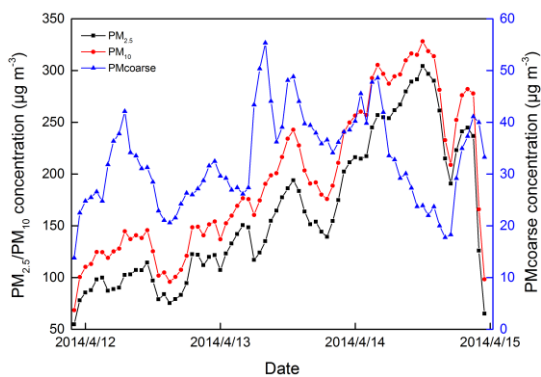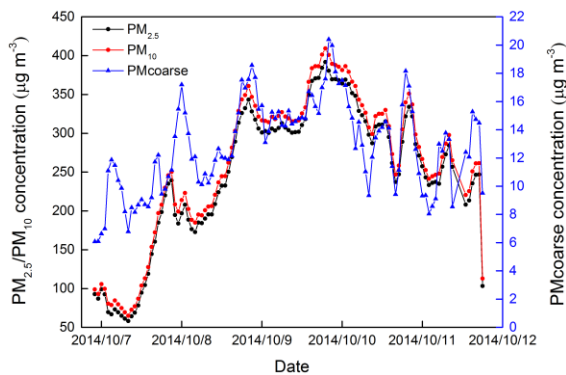
Figure A: Temporal variations of mass concentration of particulate matter observed during the whole haze event in Beijing city.

Figure B: Temporal variation of mass concentration of particulate matter observed during the whole fog–haze mixed event in Beijing city.

10. Page 12 Line 6: Why the authors did not choose the same spring season as the haze event analysis above?

Reply 10:

Thanks for the comment. The fog–haze mixed event from 22 to 28 March, 2014 for the same spring season as the haze event was much weaker and shorter-lived than that we selected (Table 1). The fog in selected fog-haze mixed case lasted about 3 days while that for the case with same season only lasted 13 hours. In order to investigate the typical long–lasting fog–haze mixed event, we chose this case. To be more clearly, we have added the message to section 3.4 of the revised manuscript as

"In all haze events, the haze event observed from 11 to 14 April was highly polluted with the maximum $PM_{2.5}$ concentration of 304 μg m^{-3} and minimum visibility of 1113 m. For all fog–haze mixed events, the fog duration was considered firstly. Two cases are chosen, in which the fog duration accounted for more than 40 % of the total. One was observed from 19 to 26 February 2014, and the other was occurred from 6 to 11 October 2014. Moreover, the maximum RH reached to 100 % in the fog–haze event occurred from 6 to 11 October 2014, which was chosen as typical fog–haze event for the following study."

Technique issue:

11. Too much figures in the manuscript, the authors may move some into supplement.

Reply 11:

Thanks for the suggestion. We have moved some figures into supplement in the revised manuscript (see Fig. S1, Fig. S2, Fig. S3 and Fig. S4 in the Supplement).

References

Cai, W., Li, K., Liao, H., Wang, H., and Wu, L.: Weather conditions conducive to Beijing severe haze more frequent under climate change, Nature Clim. Change, 7, 257-262, doi: 10.1038/nclimate3249

Chen, H., and Wang, H.: Haze Days in North China and the associated atmospheric circulations based on daily visibility data from 1960 to 2012, J. Geophys. Res. Atmos., 120, 5895-5909, doi: 10.1002/2015JD023225, 2015.

Gao, H., and Li, X.: Influences of El Nino Southern Oscillation events on haze frequency in eastern China during boreal winters, Int. J. Climatol. , 35, 2682-2688, doi: 10.1002/joc.4133, 2015.

Köhler, H.: The nucleus in and the growth of hygroscopic droplets, Transactions of the Faraday Society, 32, 1152-1161, doi: 10.1039/TF9363201152, 1936.

Li, Q., Zhang, R. H., and Wang, Y.: Interannual variation of the wintertime fog-haze days across central and eastern China and its relation with East Asian winter monsoon, Int. J. Climatol. , 36, 346-354, doi: 10.1002/joc.4350, 2016.

NOAA: Surface weather observations and reports. Federal Meteorological Handbook 94 pp, 1995.

Wang, H. J., Chen, H. P., and Liu, J. P.: Arctic Sea Ice Decline Intensified Haze Pollution in Eastern China, Atmos. Ocean. Sci. Lett., 8, 1-9, doi: 10.3878/AOSL20140081, 2015.

Xu, X., Zhao, T., Liu, F., Gong, S. L., Kristovich, D., Lu, C., Guo, Y., Cheng, X., Wang, Y., and Ding, G.: Climate modulation of the Tibetan Plateau on haze in China, Atmos. Chem. Phys., 16, 1365-1375, doi: 10.5194/acp-16-1365-2016, 2016.

Yang, Y., Liao, H., and Lou, S.: Increase in winter haze over eastern China in recent decades: Roles of variations in meteorological parameters and anthropogenic emissions, J. Geophys. Res. Atmos., 121, 13050-13065, doi: 10.1002/2016JD025136, 2016.

Yang, Y., Russell, L. M., Lou, S., Liao, H., Guo, J., Liu, Y., Singh, B., and Ghan, S. J.: Dust-wind interactions can intensify aerosol pollution over eastern China, Nat. Commun., 8, 15333, doi: 10.1038/ncomms15333, 2017a.

Yang, Y., Wang, H., Smith, S. J., Ma, P. L., and Rasch, P. J.: Source attribution of black carbon and its direct radiative forcing in China, Atmos. Chem. Phys., 17, 4319-4336, doi: 10.5194/acp-17-4319-2017, 2017b.

Zhang, R., Li, Q., and Zhang, R.: Meteorological conditions for the persistent severe fog and haze event over eastern China in January 2013, Sci. China Earth Sci., 57, 26-35, doi:10.1007/s11430-013-4774-3, 2014.

5 Zou, Y., Wang, Y., Zhang, Y., and Koo, J.: Arctic sea ice, Eurasia snow, and extreme winter haze in China, Sci. Adv., 3, doi: 10.1126/sciadv.1602751, 2017.

Manuscript # acp-2017-455
Reply to Referee #2

We are very grateful to all important and helpful comments from the referee. The followings are our responses to each comment in detail.

1. In this manuscript author reported the observation phenomena describing the tight relationship between PM and PBL in two type haze events occurred in Beijing. Facts are always important for our better understanding of the severe haze events. Authors suggest possible feedbacks among PM, PBL, and/or humidity, whereas the PBL play dominant roles. However, in the present version of the manuscript, authors just demonstrate their co-changes by correlations. The physical explanation why/how the PBL changes need careful and substantial analysis/evidence.

Reply 1:

Thanks for the suggestion. We added more explanations and discussions relevant to the PBL changes and PM concentration in conclusions and discussions section of the revised manuscript, as "The new finding in this paper has important implications in explaining the frequent long–lasting polluted events in the study region. Generally, a typical pollution event is usually formed under a stable and shallow temperature–inversion condition at low atmospheric layers, and would disappear or obviously decrease when the daytime solar radiation increases. However, in the study region, we found that many severe haze and fog–haze mixed events lasted for several days even for several weeks. Most previous publications attributed the reason as the persistent abnormal weather system or high emissions. However, this study shows that except for the influence of meteorological condition and high emission, the interactions and feedbacks between PBL and aerosol loading linked by radiation process are crucial in enhancing and maintaining these polluted events. These feedbacks could cause an important variation of dynamical/thermal processes in lower troposphere. The formation of double inversion layer and their subsequent change is closely associated with persistent meteorological condition, high aerosol loading and associated radiation process. Due to the complex interactions and feedbacks, a deeper and more stable atmospheric low–level inversion layer is formed and it is hard to break up by daytime solar radiation heating process until the strong wind occurs and removes the high aerosol loading."

2. Page 3, line 3, '…inside of the surface', misleading.

Reply 2:

Thanks for the comment. It has been changed in the revised manuscript, as "The aerosols directly emitted from polluted source and those secondly formed might be concentrated in the PBL, resulting in high concentrations near the surface."

3. Page 4, line 26, 'NCEPT', typo

Reply 3:

It has been revised as "NCEP".

4. Sections 3.1 and 3.2, as authors indicated the humidity is a very important factor modulating both the PM concentration and visibility, the relationship obtained in Section 3.1 and 3.2 would be biased by humidity. Particularly, to what extent the humidity 'contaminate' the $PM_{2.5}$-PBL and $PM_{2.5}$-visibility relationship should be clarified. It seems reasonable to perform additional analysis using data under similar humidity conditions. Otherwise the explanation would be vague.

Reply 4:

Thanks for the suggestion. We have performed additional analysis using data under similar humidity condition. The relationship between visibility and $PM_{2.5}$ mass concentrations and that between $PM_{2.5}$ mass concentration and PBL height under different RH conditions for both long–lasting haze and fog–haze mixed events are shown in Fig. A and Fig. B. The results show that the variation of RH has some influences on the relationship between $PM_{2.5}$–PBL and $PM_{2.5}$–visibility. In general, the high RH could decrease the visibility and PBL height quicker than the low RH. However, the tendency and basic conclusion are not obviously changed.
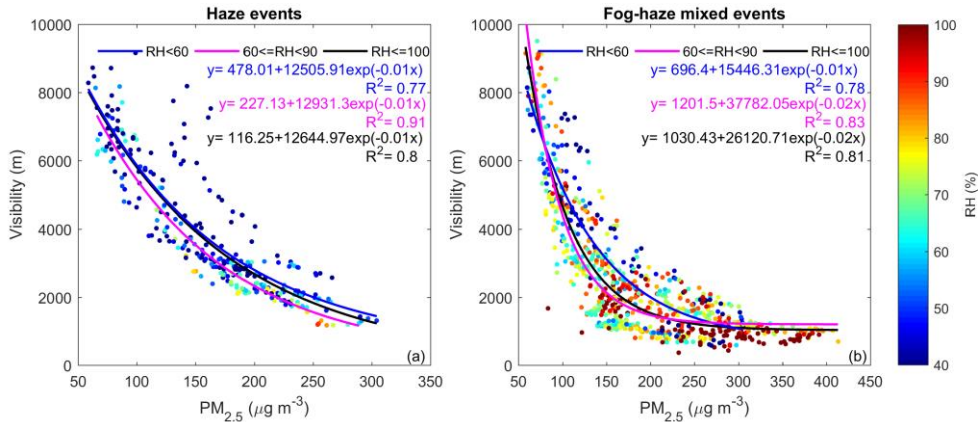

Figure A: Relationship between the measured visibility and $PM_{2.5}$ mass concentration under different RH conditions for (a) haze and (b) fog–haze mixed events from January 2014 to March 2015 in Beijing city. The exponential curves present the fits of the circles according RH.
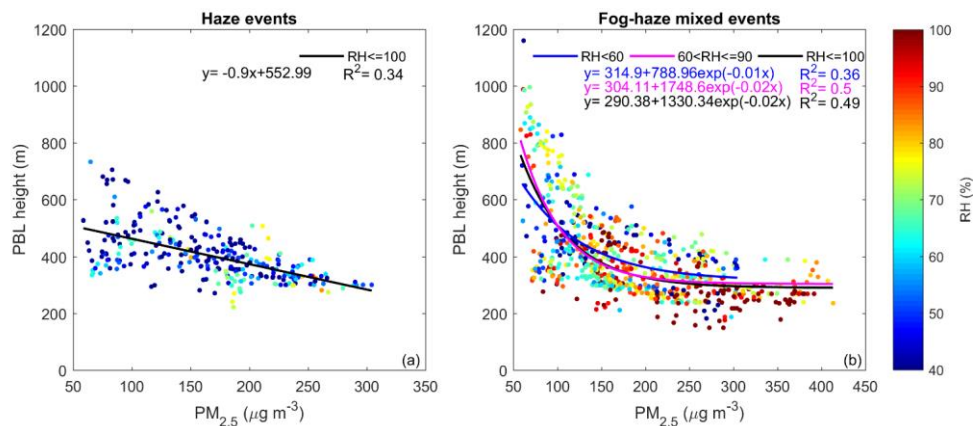
Figure B: Relationship between PBL height and PM$_{2.5}$ mass concentration under different RH conditions for (a) haze and (b) fog–haze mixed events from January 2014 to March 2015 in Beijing city. The curves present the fits of the circles according RH.

5. Page 9, line 14, 'col', typo

Reply 5:

The col pressure filed presents the pressure field of the saddle type. We rewrote the sentence in the revised manuscript as "The synoptic situation during the haze event characterized as a saddle field. Beijing was located in a saddle between two pairs of high and low pressure center."

6. Page 9, line 23, As you demonstrated, the temperature advection is important, but why the aerosol transport from the south is weak?

Reply 6:

Thanks for the comment. The sentence in the manuscript was revised as "The wind speed varied from 0 m s^{-1} to 3.9 m s^{-1}, with an average of 0.8 m s^{-1}, suggesting that the horizontal diffusion of aerosols was very weak."

7. On the PBL changes, what's the role played by the background synoptic processes? Is there any non-aerosol related dynamical/thermal causes in lower troposphere?

Reply 7:

Thank you for your comment. The background synoptic processes played an important role in the PBL changes in the cases we investigated. The upper inversion layer was formed by the persistent warm and humid airflow from south, and the PBL change was directly related to the descending process of the upper inversion layer. In the daytime, due to the existence of the

upper inversion layer, the PBL tends to become stable and aerosol loading increases. As long as the aerosol loading reach certain high value such as that larger than 150–200 μg m^{-3}, the solar radiation will be strongly blocked, and then the strong surface cooling occurs, which cause the descending of the upper layer inversion. Since the upper inversion layer contains warmer and humid air, the descending process would cause the whole PBL to be suppressed and well–mixed. These processes will finally form a deeper and more stable PBL, so the daytime radiation heating cannot break up the stable layer and cause a long–lasting pollution event until strong wind comes. We can see that the interaction and feedback between PBL and aerosol loading is linked by radiation process. We cannot find additional influence from synoptic process such as downdraft etc. Moreover, the descending process of upper inversion layer also bring more water vapour to the lower layer, high content moisture might also play an important role in blocking solar radiation except for the aerosol loading.

8. Page 12, line 1, inconvincing. It seems actually the whole layer get warmer on 13-14 April. This might help set a higher PBL.

Reply 8:

Thanks for the comment. In general, when temperature within PBL becomes higher, the PBL height should increase. However, this study shows that due to the strong cooling at the surface, the whole PBL descending and the warm PBL is caused by the descending upper warm and humid air, which is favourable to the mixing process within the PBL, but cannot force the PBL to extend upward due to the influence of strong surface cooling process caused by the rapidly increased aerosol loading. The surface cooling is higher in 14 than in 13 April 2014. For example, the inversion layer from 150 m to 550 m with the lapse rate of air temperature is –0.38 ℃ (100 m)$^{-1}$ at 8:00 on 13 April, while the lapse rate of the same layer is –0.75 ℃ (100 m)$^{-1}$ at the same time on 14 April. From the direct radiation and scattering radiation parameters in Table 3, we can also see the surface cooling effect is strengthened (the direct radiation is reduced and the scattering radiation is increased from 13 to 14 April).

9. Section 3.4.2, The PBL feedback is much stronger in fog-haze events than in haze event. This conclusion cannot be obtained, until you have ruled out the influence of synoptic processes on the PBL in these analyzed events.

Reply 9:

Thanks for the comment. This study shows that the PBL feedback is much stronger in fog–haze mixed events than in haze event. This is because that the fog–haze events include many fog droplets, which can substantially block the solar radiation comparing with aerosol loading in haze events in the daytime and cause stronger surface cooling. The stronger surface cooling would cause stronger descending of the upper inversion layer and then form a highly suppressed and more stable PBL. So the PBL feedback is much stronger in fog–haze event. As seen in Table 5 in the manuscript, the radiation reduction imposed by aerosol particles is particularly stronger during the fog–haze mixed event than the haze event. The PM$_{2.5}$ concentration is

higher and the PBL heights are lower in the fog–haze mixed event. We propose that the PBL feedback is much stronger in fog–haze mixed events than in haze event. We have added these descriptions in section 3.4.2 of the revised manuscript.

10. Page 32, The RH in Figure 10 seems not consistent with Fig.7. For example, high RH above 500m are event from 12 April to 14 April in Figure 7. But in Figure 10 (b,d) this feature cannot be found, instead, much drier conditions on 13 April and 14 April. Why?

Reply 10:

Thanks for the comment. This is primarily caused by different measuring system. Comparing with data from two methods, The RH derived from PMWR has larger uncertainties and the sounding data are more reliable. Since Fig.7 in the previous manuscript (Fig.6 in the revised manuscript) is from PMWR (Profiling microwave radiometer), which uses passive remote sensing way to obtain profiles of temperature and water vapor based on neural network algorithm with the input of past sounding data and bright temperature. So the RH values of PMWR are derived from the PMWR–retrieved temperature and water vapor density. The vertical resolution of PMWR is only 100 m for the height between 500 and 2000 m, which is not enough to obtain the fine structure of the upper boundary layer. However, the RH from PMWR has higher temporal resolution, it is still very useful compared with conventional radiosonde observation, which only has observation twice a day. In the study of (Xu et al., 2015), atmospheric profiles of RH retrieved from PMWR measurements are compared with radiosonde soundings. The correlation coefficients of RH for clear and cloudy skies are less than 0.8 and decrease monotonically with height. The biases increase from ~3 % at the surface to ~15–20 % at 4000–5000 m. It is well known that radiosonde humidity has systematic dry bias relative to the Cryogenic Frostpoint Hygrometer (Vomel et al., 2007; Bian et al., 2011).

11. Page 34, Figure 12(e), PMcorse should be PMcoarse. And how did you define PMcoarse? Should be indicated, and the relevant analysis for PMcoarse also missed in Interactive comment on Atmos. Chem. Phys. Discuss., https://doi.org/10.5194/acp-2017-455,2017.

Reply 11:

Thanks for the careful review. In the section 2.1, PMcoarse is defined as that the particulate matter with aerodynamic diameter is >2.5 μm and <=10 μm. Since the averaged $PM_{2.5}/PM_{10}$ in the haze event and fog–haze mixed event was 0.82 and 0.94, respectively. So the primary pollutant was $PM_{2.5}$ in the study region. In general, the variation trend of PMcoarse was consistent with that of $PM_{2.5}$ in both two cases. According to the above reasons, we have deleted the lines of PMcoarse in Figure 5 (e) and Figure 10 (e) in the revised manuscript.

References

Bian, J., Chen, H., Voemel, H., Duan, Y., Xuan, Y., and Lue, D.: Intercomparison of Humidity and Temperature Sensors: GTS1, Vaisala RS80, and CFH, Adv. Atmos. Sci. , 28, 139-146, 10.1007/s00376-010-9170-8, 2011.

Vomel, H., Selkirk, H., Miloshevich, L., Valverde-Canossa, J., Valdes, J., Kyro, E., Kivi, R., Stolz, W., Peng, G., and Diaz, J. A.: Radiation dry bias of the vaisala RS92 humidity sensor, J. Atmos. Ocean. Tech., 24, 953-963, 10.1175/jtech2019.1, 2007.

Xu, G. R., Xi, B. K., Zhang, W. G., Cui, C. G., Dong, X. Q., Liu, Y. Y., and Yan, G. P.: Comparison of atmospheric profiles between microwave radiometer retrievals and radiosonde soundings, Journal of Geophysical Research-Atmospheres, 120, 10313-10323, 10.1002/2015jd023438, 2015.

5

Manuscript # acp-2017-455

Reply to Referee #3

We are very grateful to all important and helpful comments from the referee. The followings are our responses to each comment in detail.

5

Summary: In this article, the authors analyzed and quantified the relationships among $PM_{2.5}$ concentration, visibility and PBL height for the haze and fog-haze mixed events using the data from several state-of-the-art instruments, and then showed the corresponding meteorological conditions for the two typical cases. Similar analyses have been implemented by many previous studies and the novelty of this study is actually not enough. However, the detailed estimations of this study can still provide

10 some valuable information for the haze early warnings. I suggest it to be accepted after several corrections. Note I am not an expert on the atmospheric chemistry, so my assessment on this part may not be accurate.

Specific comments:

1. For any journal, the first requirement is that the abstract of the article should be briefly and concisely. However, the abstract of this study is too redundant and including some valueless information that would be lowering the readability. So, this part of

15 the article is suggested to be re-worded in the next version that just the highlights from this research are needed.

Reply 1:

Thanks for the suggestion, the abstract has been re-worded in the revised manuscript, shown as below:

"The air quality and visibility are strongly influenced by aerosol loading, which is driven by meteorological conditions. The quantification of their relationships is critical to understanding the physical and chemical processes and forecasting of the

20 polluted events. We investigated and quantified the relationship among $PM_{2.5}$ (particulate matter with aerodynamic diameter is 2.5 μm and less) mass concentration, visibility and planetary boundary layer (PBL) height in this study based on the data obtained from four long–lasting haze events and seven long–lasting fog–haze mixed events from January 2014 to March 2015 in Beijing city. The statistical results show that there was a negative exponential function between the visibility and the $PM_{2.5}$ mass concentration for both haze and fog–haze mixed events. However, the fog–haze events caused a more obvious decrease

25 of visibility than that for haze events due to the formation of fog droplets that could induce higher light extinction. The $PM_{2.5}$ concentration had inversely linear correlation with PBL height for haze events and negative exponential correlation for fog– haze mixed events, indicating that the $PM_{2.5}$ concentration is more sensitive to PBL height in fog–haze mixed events. The visibility had positively linear correlation with the PBL height with the R^2 of 0.35 in haze events and positive exponential correlation with the R^2 of 0.56 in fog–haze mixed events. We also investigated the physical mechanism responsible for these

30 relationships among visibility, $PM_{2.5}$ concentration and PBL height through typical haze and fog–haze mixed event, and found that a double inversion layer formed in both typical events and played critical roles in maintaining and enhancing the long– lasting polluted events. The upper–level stable inversion layer formed by the persistent southwest warm and humid airflow

16

caused the $PM_{2.5}$ accumulation and subsequent surface cooling as well as the formation of a weak low–level inversion layer. The formation of low–level inversion layer further enhanced the $PM_{2.5}$ accumulation and surface cooling process, and induced a strong descending process of the upper–level inversion layer with warm and humid air, which significantly strengthened the PBL stability and formed a deep stable PBL in the daytime, and in return rapidly increased the $PM_{2.5}$ concentration. This positive feedback was particularly strong when the $PM_{2.5}$ mass concentration was larger than 150–200 μg m^{-3}. Therefore, the formation and subsequent descending processes of the upper–level inversion layer should be an important factor in maintaining and strengthening the long–lasting severe polluted events, which has not been revealed in previous publications. The interactions and feedbacks between $PM_{2.5}$ concentration and PBL height linked by radiation process caused an obvious and more rapid increase of $PM_{2.5}$ concentration and a significant and long–lasting deterioration of air quality and visibility in fog–haze mixed events."

2. Since 2013, increased studies have addressed the impact of climate changes on the haze pollutions over China. For example, weakened East Asian winter monsoon (Li, Qiang, et al., 2016: Interannual variation of the wintertime fog-haze days across central and eastern China and its relation with East Asian winter monsoon. Int. J. Climatol., 36, 346-354), reduced Arctic sea ice (Wang, Huijun, et al., 2015: Arctic sea ice decline intensified haze pollution in eastern China, Atmos. Oceanic Sci. Lett.,8, 1–9), Tibetan Plateau warming (Xu, X., et al., 2016: Climate modulation of the Tibetan Plateau on haze in China. Atmos. Chem. Phys., 16, 1365-1375), ENSO variability (Gao, Hui, et al., 2015: Influences of El Nino Southern Oscillation events on haze frequency in eastern China during boreal winters. Int. J. Climatol., 35, 2682-2688), etc. all showed important roles on the haze occurrences across China. I think this part of the work should be reviewed in the introduction. Additionally, there are also some studies presented the meteorological conditions for the haze pollutions from climatological perspectives (Zhang, Renhe, et al., 2014: Meteorological conditions for the persistent severe fog and haze event over eastern China in January 2013. Sci. China Earth Sci., 57, 26–35; Chen, Huopo, et al., 2015: Haze days in North China and the associated atmospheric circulations based on daily visibility data from 1960 to 2012. J. Geophys. Res. Atmos., 120, 5895-5909), which can be compared with the case analyses in this study, further increasing the readability.

Reply 2:

Thanks for the important suggestion. We have added some recent papers in the introduction section of the revised manuscript, as "In addition, the interactions between aerosol pollution and climate change have been substantially addressed in recent publications, for example, anthropogenic climate change (Cai et al., 2017), reduced Arctic sea ice (Wang et al., 2015; Zou et al., 2017), the Tibetan Plateau warming (Xu et al., 2016), influences of ENSO events on haze frequency in eastern China (Gao and Li, 2015), weakened East Asian winter monsoon (Li et al., 2016), decadal weakening of winds (Yang et al., 2016), and enhanced thermal stability of the lower atmosphere (Zhang et al., 2014; Chen and Wang, 2015). The dust–wind interaction (Yang et al., 2017a) and upwind transport (Yang et al., 2017b) could also intensify haze events in China."

3. The difference of the separating criterions of the long-lasting haze and fog-haze mixed events is the different value of minimum visibility that minimum visibility larger than 1km for haze events and smaller than 1km for fog-haze mixed events. This is the self-criterion or from the other research? The humidity is a key factor for the separation of the fog and haze events, why the relative humidity has not been considered?

Reply 3:

Thanks for the comment. As you said, the RH is critical factor for separating haze from fog events. Actually, the definition we used is from international definition of fog event. Fog is an observed horizontal visibility below 1000 m in the presence of suspended water droplets and/or ice crystals (NOAA, 1995), which means that when the horizontal visibility is below 1000 m, the fog events occur. Since the horizontal visibility for atmospheric haze event is usually larger than 1000 m, only the fog occurs the visibility can decrease to be less than 1000 m. So that is why we use the minimum visibility to define fog and haze events.

Theoretically, when a fog event occurs, the RH has to reach over 100 %. However, it is difficult to measure RH accurately, so in most cases, we use RH value of 90 % or 95 % as criterion to separate fog and haze. In fact, in the study region, when the RH is high enough, the fog and haze are usually co-existed. The haze aerosols can be transformed to fog droplets under certain conditions according to the Köhler curve (Köhler, 1936). It should be noticed that the situations such as heavy rain event or light fog events, which cause the horizontal visibility to be below or above 1000 m are not considered here. In addition, since we focus on long–lasting severe fog and haze event, we also include factors such as the lasting time and $PM_{2.5}$ mass concentration as additional criteria. To be more clearly, the corresponding text have been modified in the revised manuscript. We also revised Table 1 to include more parameters such as duration and maximum RH of the pollutant events, shown as below:

Table 1: The long–lasting haze and fog–haze mixed events from January 2014 to March 2015 in Beijing city

Type	Starting date / time	Ending date / time	Minimum visibility (m)	Duration (h)	Maximum PM$_{2.5}$ (µg m^{-3})	Maximum RH (%)	Weather phenomenon
Haze events	2014.01.21/ 15:00	2014.01.24/ 15:00	1364	73	264	68	–
	2014.04.11/ 22:00	2014.04.14/ 23:00	1113	74	304	89	–
	2015.02.12/ 21:00	2015.02.16/ 10:00	1667	86	263	77	–
	2015.03.04/ 22:00	2015.03.08/ 10:00	1886	83	266	72	–
Fog–haze mixed events	2014.02.19/ 21:00	2014.02.26/ 20:00	647	168/76[b]	269	92	02.26/16:00–21:25 Drizzle rain
	2014.03.22/ 22:00	2014.03.28/ 14:00	664	137/13[b]	417	94	3.28/4:30–6:20 Drizzle rain
	2014.10.06/ 22:00	2014.10.11/ 18:00	500	117/48[b]	391	100	10.08/6:40–7:50 10.08/10:30–11:50 Drizzle rain
	2014.10.16/ 21:00	2014.10.20/ 23:00	964	99/3[b]	322	100	–
	2014.10.22/ 4:00	2014.10.26/ 4:00	258	97/24[b]	379	100	–
	2014.10.28/ 23:00	2014.11.01/ 5:00	837	79/1[b]	184	100	10.29/23:00– 10.30/00:10 10.31/15:10–16:30 Drizzle rain
	2015.01.12/ 17:00	2015.01.16/ 3:00	526	83/8[b]	297	93[a]	01.14/10:00–10:20 snow

[a] the maximum RH of all valid data except missing measurements.
[b] fog–haze mixed event duration / fog duration.

19

4. In the context, the authors mentioned that "The PBL height derived by MPL is usually used as a reference in detecting the aerosol vertical distribution by more advanced and powerful lidars.", however, the authors also mentioned in the following paragraph that there are also some uncertainty existed for the MPL to determine the PBL height. This seems to be conflict.

Reply 4:

Thanks for the comment. Generally, MPL is a reliable tool to retrieval PBL height, however, it cannot work well in some situations such as that the aerosol concentration becomes uniform in the vertical direction (Tang et al., 2016). We revised this part based on your comment, as "The PBL heights retrieved by the attenuated backscatter profile of MPL and CL31 still exist some uncertainties (Tang et al., 2016; Geiß et al., 2017). Tang et al. (2016) founded that PBL height cannot be correctly obtained through sudden changes in the attenuated backscatter profiles. Such as in situation that the strong northerly winds with dry and clear air masses prevail in observation site, the atmospheric aerosols spread rapidly and became uniform in the vertical direction, the PBL height was substantially underestimated."

5. How about the statistical relationship between $PM_{2.5}$ ma concentration and PBL height from CL lidars?

Reply 5:

Good comment. Since MPL is much more powerful tool in retrieving PBL height, we used the data from MPL to investigate the relationship between $PM_{2.5}$ mass concentration and PBL height. When using CL data, we found that the basic relationship could be the same as that by using data from MPL, however, the correlation coefficients decreased substantially. The figure S2 below shows that the $PM_{2.5}$ concentration has inversely linear correlation with the PBL height with the R^2 of 0.2 for haze events and negative exponential correlation with the R^2 of 0.34 for fog–haze mixed events. R^2 are both lower than that determined by MPL. We have added these descriptions to section 3.2 in the revised manuscript and added Fig. S2 to the supplement.
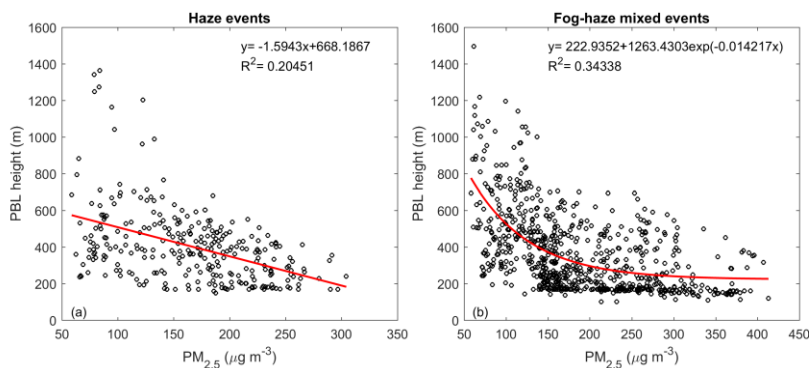

Figure S2: Relationship between PBL height derived by CL31 and $PM_{2.5}$ mass concentration for (a) haze and (b) fog–haze mixed events from January 2014 to March 2015 in Beijing city

6. In this study, the authors just showed the meteorological conditions for two typical haze events? Why chose these two cases from 11 cases? The composite analysis method is suggested for the further analysis if conveniently.

Reply 6:

Thanks for the comment. The main reason to choose two typical cases for detailed analyses is to consider their representativeness and data completeness. This study focuses on the long–lasting haze and fog–haze mixed events, we choose typical long–lasting pollutant events and also consider whether the data for these cases is complete or not. Since the most data we used in this study were observed and supported by just a research project, it is not an easy thing to maintain these advanced instruments and obtain a complete data case from its occurrence to the end.

We have added some descriptions for this comment in the revised manuscript, as "To clarify the physical mechanism responsible for the relationship among $PM_{2.5}$, visibility and PBL height obtained above, two typical cases of long–lasting haze and fog–haze mixed events are presented and further investigated in considering their representativeness and data completeness of all cases (Table 1). In all haze events, the haze event observed from 11 to 14 April, 2014 was highly polluted with the maximum $PM_{2.5}$ concentration of 304 μg m^{-3} and minimum visibility of 1113 m. For all fog–haze mixed events, the fog duration was considered firstly. Two cases are chosen, in which the fog duration accounted for more than 40 % of the total. One was observed from 19 to 26 February 2014, and the other was occurred from 6 to 11 October 2014. The maximum $PM_{2.5}$ concentration was more higher and the maximum RH reached to 100% in the fog–haze event occurred from 6 to 11 October 2014, which was chosen as typical fog–haze event for the following study."

7. The authors presented detailed analyses on the meteorological conditions for the long-lasting haze and fog-haze mixed events. However, I am still not clear what the difference for the meteorological conditions between these two cases. So, the comparison discussion in this aspect should be added in the section of Conclusion and Discussions, not just showing the common features as the current MS did.

Reply 7:

Thanks to the referee for the suggestion. The main differences of meteorological condition for two cases are humidity and duration. Although both cases occurred in a stable weak pressure field covering northern China, the haze event was relatively drier with shorter duration while the fog–haze mixed event was highly humid with longer duration. Since the fog droplets was formed in the fog–haze mixed event, the radiation reduction at surface was more obvious and stronger, which caused stronger descending process of the upper inversion layer, and formed a more stable PBL.

Based on your comment, we added some descriptions relevant to the differences of meteorological conditions between two cases in the section of conclusions and discussions in the revised manuscript, as "The main differences of meteorological condition for two cases are humidity and duration. Although both cases occurred in a stable weak pressure field covering northern China, the haze event was drier and duration was shorter while the fog–haze mixed event was more humid and had a longer duration. Since the fog droplets were formed in the fog–haze mixed event, the radiation reduction at surface was more

obvious and stronger, and caused stronger descending process of the upper inversion layer. In most cases, light precipitation (drizzle rain or light snow) occurred during the fog–haze mixed event while in all haze events during the observation period, there was no precipitation. The fog–haze mixed event was more favorable to form extremely high mass concentration of $PM_{2.5}$ (>300 μg m^{-3}) than the haze event."

8. To increase the readability, the location of Beijing is suggested to be highlighted in Figure 11 and 17.

Reply 8:

Thanks for the suggestion. The location of Beijing has been added in the Fig.S3 and Fig.S4 in the revised manuscript. The revised figures are shown as below:
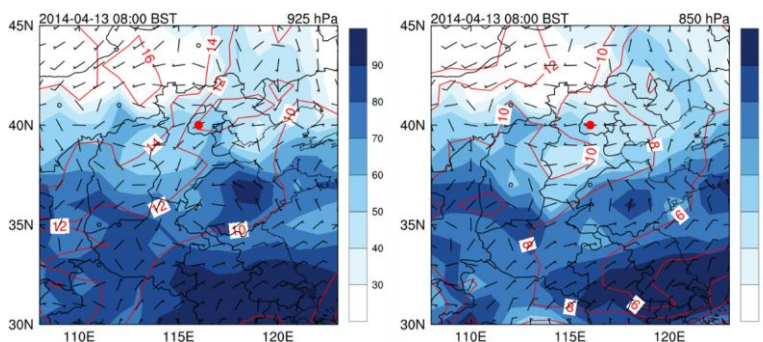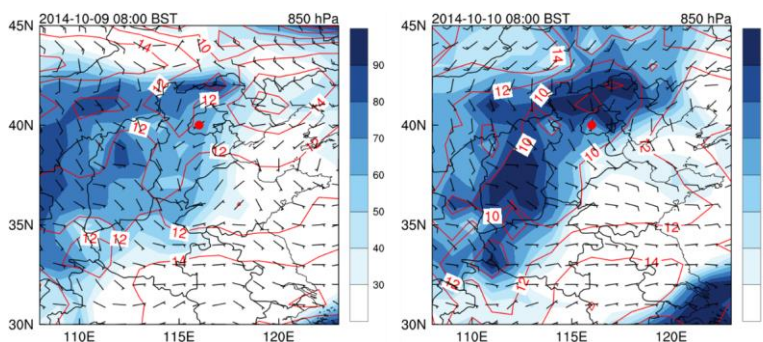

Figure S3: Temperature (red contour lines, units: ℃), RH (color shading, units: %) and wind (wind bar) distribution in (a) 925 hPa and (b) 850 hPa at 08:00 BST on 13 April 2014. The red dot represents the site of CMA

Figure S4: Temperature (red contour lines, units: ℃), RH (color shading, units: %) and wind (wind bar) distribution in 850 hPa at 08:00 BST on (a) 9 October and (b) 10 October 2014. The red dot represents the site of CMA.

References

Cai, W., Li, K., Liao, H., Wang, H., and Wu, L.: Weather conditions conducive to Beijing severe haze more frequent under climate change, Nature Clim. Change, 7, 257-262, doi: 10.1038/nclimate3249

Chen, H., and Wang, H.: Haze Days in North China and the associated atmospheric circulations based on daily visibility data from 1960 to 2012, J. Geophys. Res. Atmos., 120, 5895-5909, doi: 10.1002/2015JD023225, 2015.

Gao, H., and Li, X.: Influences of El Nino Southern Oscillation events on haze frequency in eastern China during boreal winters, Int. J. Climatol. , 35, 2682-2688, doi: 10.1002/joc.4133, 2015.

Geiß, A., Wiegner, M., Bonn, B., Schäfer, K., Forkel, R., von Schneidemesser, E., Münkel, C., Chan, K. L., and Nothard, R.: Mixing layer height as an indicator for urban air quality?, Atmos. Meas. Tech., 10, 2969-2988, doi:10.5194/amt-10-2969-2017, 2017.

Köhler, H.: The nucleus in and the growth of hygroscopic droplets, Transactions of the Faraday Society, 32, 1152-1161, doi: 10.1039/TF9363201152, 1936.

Li, Q., Zhang, R. H., and Wang, Y.: Interannual variation of the wintertime fog-haze days across central and eastern China and its relation with East Asian winter monsoon, Int. J. Climatol. , 36, 346-354, doi: 10.1002/joc.4350, 2016.

Liu, Q., Sheng, L., Cao, Z., Diao, Y., Wang, W., and Zhou, Y.: Dual effects of the winter monsoon on haze-fog variations in eastern China, Journal of Geophysical Research-Atmospheres, 122, 5857-5869, doi:10.1002/2016jd026296, 2017.

NOAA: Surface weather observations and reports. Federal Meteorological Handbook 94 pp, 1995.

Tang, G. Q., Zhang, J. Q., Zhu, X. W., Song, T., Münkel, C., Hu, B., Schäfer, K., Liu, Z. R., Zhang, J. K., Wang, L. L., Xin, J. Y., Suppan, P., and Wang, Y. S.: Mixing layer height and its implications for air pollution over Beijing, China, Atmos. Chem. Phys., 16, 2459-2475, doi:10.5194/acp-16-2459-2016, 2016.

Wang, H. J., Chen, H. P., and Liu, J. P.: Arctic Sea Ice Decline Intensified Haze Pollution in Eastern China, Atmos. Ocean. Sci. Lett., 8, 1-9, doi: 10.3878/AOSL20140081, 2015.

Xu, X., Zhao, T., Liu, F., Gong, S. L., Kristovich, D., Lu, C., Guo, Y., Cheng, X., Wang, Y., and Ding, G.: Climate modulation of the Tibetan Plateau on haze in China, Atmos. Chem. Phys., 16, 1365-1375, doi: 10.5194/acp-16-1365-2016, 2016.

Yang, Y., Liao, H., and Lou, S.: Increase in winter haze over eastern China in recent decades: Roles of variations in meteorological parameters and anthropogenic emissions, J. Geophys. Res. Atmos., 121, 13050-13065, doi: 10.1002/2016JD025136, 2016.

Yang, Y., Russell, L. M., Lou, S., Liao, H., Guo, J., Liu, Y., Singh, B., and Ghan, S. J.: Dust-wind interactions can intensify aerosol pollution over eastern China, Nat. Commun., 8, 15333, doi: 10.1038/ncomms15333, 2017a.

Yang, Y., Wang, H., Smith, S. J., Ma, P. L., and Rasch, P. J.: Source attribution of black carbon and its direct radiative forcing in China, Atmos. Chem. Phys., 17, 4319-4336, doi: 10.5194/acp-17-4319-2017, 2017b.

Zhang, R., Li, Q., and Zhang, R.: Meteorological conditions for the persistent severe fog and haze event over eastern China in January 2013, Sci. China Earth Sci., 57, 26-35, doi:10.1007/s11430-013-4774-3, 2014.

Zou, Y., Wang, Y., Zhang, Y., and Koo, J.: Arctic sea ice, Eurasia snow, and extreme winter haze in China, Sci. Adv., 3, doi: 10.1126/sciadv.1602751, 2017.

Quantifying the relationship among PM$_{2.5}$ concentration, visibility and planetary boundary layer height for long–lasting haze and fog–haze mixed events in Beijing city

Tian Luan[1,2], Xueliang Guo[1,2,3], Lijun Guo[1,2], Tianhang Zhang[4]

5 [1]State Key Laboratory of Severe Weather (LASW), Chinese Academy of Meteorological Sciences, Beijing, 100081, China
[2]Key Laboratory for Cloud Physics, Chinese Academy of Meteorological Sciences, Beijing, 100081, China
[3]Collaborative Innovation Center for Meteorological Disasters Forecast, Early Warning and Assessment, Nanjing University of Information Science and Technology, Nanjing, 210044, China
[4]National Meteorological Center, Beijing, 100081, China

10 *Correspondence to*: Xueliang Guo (guoxl@camscma.cn)

Abstract. The air quality and visibility are strongly influenced by aerosol loading, which is driven by meteorological conditions. The quantification of their relationships is critical to understanding the physical and chemical processes and forecasting of the polluted events. We investigated and quantified the relationship among PM$_{2.5}$ (particulate matter with aerodynamic diameter is 2.5 μm and less) mass concentration, visibility and planetary boundary layer (PBL) height in this

15 study based on the data obtained from four long–lasting haze events and seven fog–haze mixed events from January 2014 to March 2015 in Beijing city. The statistical results show that there was a negative exponential function between the visibility and the PM$_{2.5}$ mass concentration for both haze and fog–haze mixed events (with the same R^2 of 0.80). However, the fog–haze events caused a more obvious decrease of visibility than that for haze events due to the formation of fog droplets that could induce higher light extinction. The PM$_{2.5}$ concentration had inversely linear correlation with PBL height for haze events and

20 negative exponential correlation for fog–haze mixed events, indicating that the PM$_{2.5}$ concentration is more sensitive to PBL height in fog–haze mixed events. The visibility had positively linear correlation with the PBL height with the R^2 of 0.35 in haze events and positive exponential correlation with the R^2 of 0.56 in fog–haze mixed events. We also investigated the physical mechanism responsible for these relationships among visibility, PM$_{2.5}$ concentration and PBL height through typical haze and fog–haze mixed event, and found that a double inversion layer formed in both typical events and played critical roles

25 in maintaining and enhancing the long–lasting polluted events. The upper–level stable inversion layer formed by the persistent southwest warm and humid airflow caused the PM$_{2.5}$ accumulation and subsequent surface cooling as well as the formation of a weak low–level inversion layer. The formation of low–level inversion layer further enhanced the PM$_{2.5}$ accumulation and surface cooling process, and induced a strong descending process of the upper–level inversion layer with warm and humid air, which significantly strengthened the PBL stability and formed a deep stable PBL in the daytime, and in return rapidly increased

30 the PM$_{2.5}$ concentration. This positive feedback was particularly strong when the PM$_{2.5}$ mass concentration was larger than 150–200 μg m^{-3}. Therefore, the formation and subsequent descending processes of the upper–level inversion layer should be an important factor in maintaining and strengthening the long–lasting severe polluted events, which has not been revealed in previous publications. The interactions and feedbacks between PM$_{2.5}$ concentration and PBL height linked by radiation process

25

caused an obvious and more rapid increase of $PM_{2.5}$ concentration and a significant and long–lasting deterioration of air quality and visibility in fog–haze mixed events.

1 Introduction

Due to a rapid economic development, the haze and fog events characterized by the high fine particulate matter (i.e. $PM_{2.5}$, particulate matter with aerodynamic diameter is 2.5 μm and less) levels have occurred during the last few decades in China, especially in the most developed and high–populated city (Chan and Yao, 2008; Zhang et al., 2013; Huang et al., 2014; Zhang and Cao, 2015). For instance, in January 2013, Beijing (and the entire inland China) suffered from the extremely severe and persistent haze and fog pollution, registering the highest $PM_{2.5}$ hourly concentration of 886 µg m^{-3} (Zhang et al., 2013; H. Wang et al., 2014; Zhang et al., 2014). The high frequency of extremely severe and persistent haze and fog events in China leads to a high public concern due to its poor visibility and adverse health effects (Tie et al., 2009; Chen et al., 2013; Pope and Dockery, 2013; Di et al., 2017), and climate change impacts (Qian et al.,2006; Liao et al., 2015).

Aerosol particles and fog droplets are responsible for the reduction of visibility by scattering and absorbing light, according to their number and properties, such as size, shape, and chemical composition. Atmospheric humidity is a major factor affecting the particle properties, as aerosols can grow by the uptake of water. When relative humidity (RH) is larger than 95 %, the atmospheric visibility can be critically reduced (Chen et al., 2012). When RH is larger than 100 %, some of the hygroscopic aerosols can be activated and form fog droplets (Pruppacher and Klett, 1978). The sudden increase in particle size causes a sharp drop in visibility, usually to distances below 1000 m (Elias et al., 2009). Baumer et al. (2008) found that the visibility decrease was associated with a continuous increase in the number size distribution of particles with diameters larger than 300 nm in South–West Germany. Particles have grown into a size interval in which their diameter is of the same order as the wavelength of the visible light, which leads to a more effective light scattering. Therefore, the visibility should decrease.

Large emission sources emit primary aerosols and the precursors of secondary aerosols, resulting in high loads of aerosols (i.e. sulfate, nitrate, ammonium, black carbon, organic carbon, and dust) (Zhang et al., 2009; Zhang et al., 2012; Zhang et al., 2013). This is the main reason for the deterioration of visibility and frequent haze events through light extinction (Cao et al., 2012; Han et al., 2016). During the haze periods, the concentration of particulate matter is much higher than that on normal days, and fine–mode aerosols are predominant (Quan et al., 2011; Zhang and Cao, 2015). Han et al. (2016) found that the 71±17 % of PM_{10} was $PM_{2.5}$ in Beijing and the increasing of $PM_{2.5}$ contributed to visibility impairment significantly.

In addition, the interactions between aerosol pollution and climate change have been substantially addressed in recent publications, for example, anthropogenic climate change (Cai et al., 2017), reduced Arctic sea ice (Wang et al., 2015; Zou et al., 2017), the Tibetan Plateau warming (Xu et al., 2016), influences of ENSO events on haze frequency in eastern China (Gao and Li, 2015), weakened East Asian winter monsoon (Li et al., 2016), decadal weakening of winds (Yang et al., 2016), and enhanced thermal stability of the lower atmosphere (Zhang et al., 2014; Chen and Wang, 2015). The dust–wind interaction (Yang et al., 2017a) and upwind transport (Yang et al., 2017b) could also intensify haze events in China.

Fog and haze events usually occur in the stable PBL, which is located at the lowest atmospheric layer and strongly influenced by the exchange of momentum, heat, and water vapor at the earth's surface. Many previous publications showed that fog and haze events were usually formed in a weak high–pressure system with low surface wind, which was unfavourable for air mixing and pollutants diffusion (Liu et al., 2007; Kang et al., 2013; X. J. Zhao et al., 2013; G. J. Zheng et al., 2015). The aerosols directly emitted from polluted source and those secondly formed might be concentrated in the PBL, resulting in high concentrations near the surface. Sun et al. (2013) suggested that the $PM_{2.5}$ distribution depicted a "higher–bottom and lower–top" pattern based on the observation of the 325 m tower in Beijing. Zhang and Cao (2015) showed that the $PM_{2.5}$ concentration at night was about 2 times higher than that in the afternoon. The lowest concentrations were observed in afternoon hours when the PBL height became larger and wind speed increased. Many studies also found that the diurnal variation of the pollutants was anti–correlated with the diurnal variation of PBL height (Chou et al., 2007; Boyouk et al., 2010). Yang et al. (2013) indicated that one of the possible factors leading to the deteriorated air quality in Hong Kong was the decreasing trend of the daily maximum of mixing layer height based on 6.5 y measurements.

Interactions among aerosols, radiation and atmospheric boundary layer structure are very complex processes and still uncertain in many aspects. Aerosols such as black carbon can strongly absorb solar radiation and modify the vertical profile of temperature in the atmosphere and stabilize the PBL structure (Ding et al., 2016). The accumulation of aerosols in the PBL can lead to a more stable atmosphere. Analysis of a heavy pollution episode in fall 2004 over northern China showed that the instantaneous irradiance at the surface decreased by about 350 W m^{-2} and the atmospheric solar heating was about 300 W m^{-2}; therefore, a more stable atmosphere was expected (Liu et al., 2007). Quan et al. (2013) found that the heat flux of surface and PBL height in haze condition were significantly lower than that under clear sky condition, and proposed that the feedback might exist between PBL height and aerosol loading. The enhancement of aerosols tends to depress the development of PBL by decreasing solar radiation, while the repressed structure of PBL will in turn weak the diffusion of pollutants, leading to the heavy pollution.

The model results from Gao et al. (2015) showed that during the fog and haze mixed event over the North China Plain, aerosols led to a significant negative radiation forcing at the surface and a large positive radiation forcing in the atmosphere and induced significant changes in meteorological variables in day time. As a result, atmosphere was much more stable and thus the surface wind speed decreased and the PBL height decreased. The maximum increase of hourly surface $PM_{2.5}$ concentration was 50 μg m^{-3} over Beijing. J. Wang et al. (2014) implied that the interaction between aerosol and radiation played an important role in the haze episode in January 2013 from simulated results by WRF–CMAQ. Petäjä et al. (2016) showed that aerosol–boundary layer feedback remained moderate at fine particular matter concentrations lower than 200 μg m^{-3}, but that it became increasingly effective at higher particular matter loadings resulting from the combined effect of high surface particular emissions and massive secondary particular matter production within boundary layer.

The influence of convective mixing on the air quality has been recognized for decades, yet data showing this phenomenon remain rather limited for the lack of temporal resolution in the PBL height measurement. The development and application of lidar have made such an investigation possible. The lidar technique has provided a useful tool to investigate cloud and aerosol

27

properties with high temporal resolution in the atmosphere (Welton et al., 2002; Y. W. Zhang et al., 2015). It is also known to be suitable for studying the PBL and its evolution (Yan et al., 2013; Zhang et al., 2016). Micro Pulse Lidar (MPL) systems were used to measure aerosol properties during the Indian Ocean Experiment (INDOEX) 1999 field phase (Welton et al., 2000, 2002). Chen et al. (2001) observed seasonal changes of the mixing layer height in Japan by using the MPL. He et al. (2008) analysed aerosol vertical distribution in the lower troposphere by examining the aerosol extinction profiles derived from MPL measurements in Hong Kong. Yang et al. (2013) analysed the diurnal, seasonal and inter–annual variation of PBL height from 6.5 y lidar data set over Hong Kong. Y. W. Zhang et al. (2015) showed the evolution of aerosol vertical distribution and the PBL height during the haze events in Shanghai.

Although there have been many theoretical and observational studies on the characteristics of $PM_{2.5}$ concentration, visibility and PBL height as well as their correlations, the quantitative investigations on their relationship for long–lasting haze and fog–haze mixed events are few. The feedback mechanism between $PM_{2.5}$ concentration and PBL height has not been well understood. Since 2013, a comprehensive field campaign on haze and fog–haze mixed events had been conducted in northern China. The state–of–the–art instruments such as Micro Pulse Lidar (MPL), ceilometer (CL31), profiling microwave radiometer (PMWR), and particulate monitor as well as some conventional meteorological instruments have been used in this field campaign. The data were acquired during the long–lasting pollutant events from January 2014 to March 2015. In this study, the relationship among $PM_{2.5}$, visibility and PBL height for both haze and fog–haze mixed events were investigated and quantified. The physical mechanism responsible for their relationships and feedbacks were also investigated and discussed.

2 Methodologies

2.1 Observational site and instruments

The observational site is located at the campus of China Meteorological Administration (CMA) (39°57′ N, 116°20′ E) in Beijing city, northern China. It was built on the roof of a 20 m tall building from the year of 2013, which located in the northwest part of urban Beijing, close to the West 3th Ring Road, without any major sources nearby. Data used in this study include the mass concentration of $PM_{2.5}$, visibility and the PBL height obtained from ceilometer, as well as the temperature, RH, water vapor and liquid profiles retrieved by PMWR. The vertical profiles of aerosol in the troposphere, and the PBL height were also obtained from a ground–based MPL installed in a working container 10 m far away from the building at the campus of CMA. The meteorological parameters (surface wind, ambient temperature and RH) were obtained from Haidian automatic weather station. Radiosonde sounding data (twice a day at 08:00 and 20:00 LST (Local Standard Time)) and daily radiation data were obtained from Beijing Meteorological station (39°56′ N, 116°17′ E, 54511). These measurement sites are located within distances of 30 km each other, as shown the sketch map of Fig. 1. NCEP FNL (Final) Operational Global Analysis data were used to analyse the meteorological factors and weather patterns. The data on 1 degree by 1 degree grids prepared operationally every six hours.

删除的内容: ;

删除的内容: T

Micro Pulse Lidar (MPL–4B) (Sigma Space Corporation, USA) is a portable eye–safe elastic backscatter lidar, fully automated. It can work 24 h per day outdoors in an unattended mode under almost any weather conditions. The laser light source is a diode–pumped frequency–doubled solid–state laser (Nd: YVO_4 at 532 nm) yielding pulsed visible green light. The pulse repetition frequency is 2500 Hz. The peak value of the optical energy of laser beam is 10 μJ. The pulse duration was set to 100

5   ns, and the pulse interval was set to 200 ns, corresponding to a vertical resolution of 30 m. Before processing the lidar data, the raw signal needed correction including optical overlap, after pulse, dead time, and background noise correction (Campbell et al., 2002, 2008). Then the aerosol optical properties can be retrieved by the lidar equations using Fernald algorithm (Fernald, 1984). The lidar signal is not available in the first hundred meters because of after pulse effect. The lowest sounding height was set to 100 m.

10   Ceilometer used in this study is a Vaisala CL31 model, described in detail in Münkel and Räsänen (2004) and Münkel et al. (2007). In brief, CL31 is equipped with an indium gallium arsenide/ metal–organic chemical vapor deposition (InGaAs/MOCVD) pulsed diode laser emitting at 905±10 nm and having an energy per pulse of 1.2 μJ±20 %. The emission frequency is 10 kHz, while the pulse duration is 110 ns. According to the Vaisala ceilometer CL31 User's Guide (2009), the full overlap of the instrument is achieved for altitudes higher than 10 m, although in practice on the order of 70 m (Martucci

15   et al., 2010). The attenuated backscatter coefficient is obtained from 10 m to 7500 m height, with a selectable spatial resolution of 5 or 10 m and temporal resolution of 2 s to 120 s. In this study, we used 10 m raw range resolution and 16 s raw temporal resolution. This temporal resolution was deemed sufficient for analysing the development of PBL structure. Apart from the very strong backscatter from clouds and fogs, the weaker gradients of the backscatter intensity were mainly determined by the number and the size spectrum of aerosol particles suspending in the air.

20   TEOM 1405–DF particulate monitor (Tapered Element Oscillating Microbalance, Thermo Fisher Scientific, USA) was used to continuously measure particulate matter mass concentration. According to the TEOM 1405–DF Operating Guide (2009), the monitor draws ambient air through two TEOM filters at constant flow rate, continuously weighing the filters and calculating near real–time mass concentrations of both $PM_{2.5}$ and PMcoarse (2.5 μm <particulate matter with aerodynamic diameter <=10 μm). By adding these two values, the PM_{10} mass concentration is obtained. The FDMS unit dries the sample flow and

25   automatically generates mass concentration measurement that account for both nonvolatile and volatile particulate matter components. The volatile faction of the collected sample is automatically compensated by using a switching valve to change the path of the fine and coarse sample flows every 6 min. The filters were replaced when the filter loading percentage nears 100 %.

Profiling microwave radiometer (PMWR–3069A, Radiometrics Co., USA) collects atmospheric radiation measurements in

30   the 20 to 200 GHz region to retrieve temperature, RH, water vapor and liquid profiles. The temperature profiling subsystem utilizes sky brightness temperature observations at selected frequencies between 51 and 59 GHz. The water vapor profiling subsystem utilizes sky brightness temperature observations at selected frequencies between 22 and 30 GHz. The water vapor channels are calibrated by means of tipping curves; the temperature channels are calibrated by a liquid nitrogen cold target. The temperature, RH, vapor density and liquid water content (LWC) profiles in this study are retrieved from PMWR

删除的内容: ;

删除的内容: 7.5 km

measurements at zenith direction. The temporal resolution of 2–3 min, and the vertical resolutions of 50 m from the surface to 500 m, 100 m from 500 m to 2000 m, and 250 m from 2000 m to 10000 m. The accuracy of MWR profiles is compatible with most meteorology applications, especially in the lower troposphere (Cimini et al., 2011; Ware et al., 2013; Gultepe et al., 2015). The visibility sensor (PWD20, Vaisala Co., Finland) with range of 10–20,000 m was employed to monitor atmospheric visibility.

2.2 Determination of the PBL height

The PBL height is determined at the altitude where a sudden decrease in the scattering coefficient occurs. In this paper, we used the wavelet covariance transform method by Brooks (2003) to inverse the PBL height by MPL, which is based on scanning the backscatter profile with a localized impulse function and maximizing the covariance between the backscatter profile and impulse function. A step function Haar wavelet is defined as Eq. (1):

$$h\left(\frac{z-b}{a}\right) = \begin{cases} +1: & b - \frac{a}{2} \le z \le b \\ -1: & b \le z \le b + \frac{a}{2} \\ 0: & elsewhere \end{cases} \tag{1}$$

where z is altitude, b is the location at which the Harr function is centered, and a is the spatial extent of the function. The covariance transformation of the Haar function (W_f) is calculated by Eq. (2):

$$W_f(a,b) = \frac{1}{a}\int_{z_b}^{z_t} f(z) \, h\left(\frac{z-b}{a}\right) dz \tag{2}$$

where $f(z)$ is the signal of the MPL backscatter profile, and z_b and z_t are the lower and upper limits of the profile. A local maximum in $W_f(a,b)$ identifies a step in $f(z)$, located at $z=b$. b is the top of the PBL.

Ceilometer is a robust low–power, low–cost and low–maintenance Lidar designed to determine the cloud base height but also provide the backscatter profile, though with less sensitivity than a Lidar. Several studies have proposed that ceilometer–measured backscatter profiles can be used to derive the PBL height (Eresmaa et al., 2006, 2012; Münkel, 2007; Haeffelin et al., 2012; Schween et al., 2014). "Structure of the atmosphere" (STRAT–2D) algorithm was selected for estimating the PBL height, which was proposed in the literatures (Morille et al., 2007; Haeffelin et al., 2012; Wiegner et al., 2014). To eliminate the influence of inherent noise and aerosol layers on the data, spatial and temporal averaging must be carried out before the gradient method used to calculate the PBL height. In this paper, the settings use 80 m height averaging close to the ground. This interval is gradually increased to 360 m averaging used at heights above 1500 m. Time averaging is dependent on the current signal noise. It varies between 14 min during nighttime and 52 min on a bright, cloudy day (Tang et al., 2016). This method uses the vertical aerosol backscatter gradient, whereby strong negative gradients can indicate the PBL height. STRAT–2D determines three candidates for PBL height: the largest, the second largest gradient and the lowest height gradient.

删除的内容: 2 km

删除的内容: 2 km

删除的内容: 10 km

删除的内容: Eresmaa et al., 2012;

2.3 Data processing

In the previous studies, the fog–haze pollution was defined as a phenomenon in which a visibility is less than 10000 m resulted from the dense accumulation of fine aerosol particles (Fu and Chen, 2017; Liu et al., 2017; Li et al., 2016). Here, we further divided the studied cases into haze events and fog–haze mixed events. According to the Kohler curve (Köhler, 1936), the haze aerosols can be transformed to fog droplets under certain meteorological conditions. The classification is usually done based on values of the visibility range (Cho et al., 2000; Tardif and Rasmussen, 2007; Elias et al., 2009). The international definition of a fog event is an observed horizontal visibility below 1000 m in the presence of suspended water droplets and/or ice crystals (NOAA, 1995). However, the fog droplets and haze aerosols are usually mixed and co-existed in the polluted region. In this study, if the fog occurred in the pollutant episode, it was defined as the fog–haze mixed event, which is similar as the study in Sun et al. (2006). If the fog did not occur in the whole pollutant episode, it was defined as the haze event. Since our study focuses on long–lasting haze and fog–haze mixed events, the parameters of the PM$_{2.5}$ concentration (>=50 µg m^{-3}) and lasting–time (>= 72 hours) of these events were included as additional criteria. It should be noticed that the situations such as heavy rain event or light fog events, which cause the horizontal visibility to be below or above 1000 m are not considered here. From January 2014 to March 2015, the total number of persistent pollutant cases is 11, in which four haze cases and seven fog–haze mixed cases were obtained. Table 1 listed all cases investigated. The RH in each haze event was lower than 90 %. The maximum RH of each haze event was 68 %, 89 %, 77 % and 72 %, respectively. The maximum RH of each fog–haze mixed event was larger than 90 %. The results were consistent with the study of Xu et al. (2016) and Q. Zhang et al. (2015), in which the observed RH less than 90 % was used to separate haze events from fog events under the visibility<10000 m due to the difficulty to measure RH correctly.

3 Results and discussion

3.1 Relationship between visibility and PM$_{2.5}$ mass concentration

Previous studies indicated that the increase in PM$_{2.5}$ mass concentration contributed to visibility impairment significantly in China (Cao et al., 2012; Han et al., 2013; H. J. Zhao et al., 2013; Li et al., 2015; Han et al., 2016). The relationships between visibility and PM$_{2.5}$ mass concentrations for both long–lasting haze and fog–haze mixed events are shown in Fig. 2, and the corresponding regression results are given in Table 2. It shows that there is a negative exponential function between the visibility and the PM$_{2.5}$ mass concentration for both haze and fog–haze mixed events with the same R^2 of 0.80. The relationship for haze events is consistent with the previous result of Han's study on the relationship between daily averaged PM$_{2.5}$ concentration and visibility under stable meteorological condition from October 2013 to September 2014 at Beijing. However, the fog–haze mixed events could cause greater visibility impairments, for example, in the haze events, the visibility reduced from 5800 to 2700 m as the PM$_{2.5}$ concentration increased from 100 to 200 µg m^{-3}, and in the fog–haze mixed events the visibility reduced from 4700 to 1500 m for the same amount of PM$_{2.5}$ concentration increase. The differences between the two

31

删除的内容: In this work, the criterions of long–lasting haze and fog–haze mixed events were defined as: (1) for the long–lasting haze events, the following conditions should be satisfied: 1 km < hourly visibility and minimum visibility <=10 km and the hourly PM$_{2.5}$ concentration >=50 µg m^{-3} for lasting more than 72 hours continuously. (2) for the long–lasting fog–haze mixed events, the following conditions need to be satisfied: minimum visibility <=1 km, hourly visibility <=10 km and the hourly PM$_{2.5}$ concentration >=50 µg m^{-3} for lasting more than 72 hours continuously.

删除的内容: a

删除的内容: was

删除的内容: 5.8

删除的内容: 2.7 km

删除的内容: 4.7

删除的内容: 1.5 km

conditions are mainly due to the increase of RH and the formation of fog droplets that could induce higher light extinction. The averaged RH observed by Haidian automatic weather station in haze and fog–haze mixed events is 46.7 % and 74.6 %, respectively. Under high RH conditions, a large amount of water vapor coated on water–soluble particle surface, enlarges the particle size, which significantly enhances the particulate light scattering efficiency and deteriorates visibility. When water vapor saturated, haze aerosols could be activated to form fog droplets, which led to the further decrease of visibility (Elias et al., 2009; Klein and Dabas, 2014; Guo et al., 2015).

Moreover, in the aqueous phase, the production rate of sulfate and nitrate aerosols was enhanced by aqueous–phase chemistry (i.e., in–fog oxidation by dissolved ozone (O_3) and hydrogen peroxide (H_2O_2)) (Andreae and Rosenfeld, 2008; Seinfeld and Pandis, 2012) and heterogeneous chemistry (Pandis et al., 1992; B. Zheng et al., 2015; G. J. Zheng et al., 2015). Sulfur oxidation ratios showed a rapid increase as a function of RH, which varied from ~0.05 at RH < ~40 % to 0.2 at RH = ~80 % and greatly increased to 0.4 via aqueous–phase processing (Sun et al., 2014). Han et al. (2013) showed that sulfate and nitrate were the two major inorganic aerosol components of $PM_{2.5}$ in Beijing that evidently decreased visibility by contributing 40–45 % to the total extinction coefficient value. Cao et al. (2012) indicated that high secondary inorganic aerosol (i.e. SO_4^{2-} and NO_3^-) were the main contributors for visibility <5000 m. Kang et al. (2013) indicated that aerosol concentration in the diameter from 0.6 to 1.4 µm increased dramatically and mainly attributed to the remarkable increase of scattering coefficient and decrease of visibility in a long–lasting haze in Nanjing. Shi et al. (2014) addressed the relationship of visibility with PM_1 and total water–soluble ions during the periods of December 2012. They found that hourly total water–soluble ions mass concentration had a better correlation with visibility, and the formation / dissociation of NH_4NO_3 and NH_4Cl exerted great impacts on visibility. Strong NH_3 and HNO_3 reaction resulted in the enhancement of NH_4NO_3 mass fraction under high RH condition that contributed to visibility degradation.

3.2 Relationship between $PM_{2.5}$ mass concentration and PBL height

The PBL height can be derived from both MPL and CL31 instruments. Figure S1 shows the PBL height determined by MPL versus that by CL31, and the 1:1 line is given for reference. The figure reveals R^2=0.70 with differences between −408 m and 692 m. The number of the difference of PBL height retrieved by MPL and CL31 within ± 300 m accounts for 97 % of the total. Tsaknakis et al. (2011) obtained that the differences of PBL height derived by Raymetrics lidar and CL31 were about 50–100 m based on the two cases in the midday. This difference may be attributed mainly to the different wavelengths used by MPL and CL31. The PBL height derived by MPL is usually used as a reference in detecting the aerosol vertical distribution by more advanced and powerful lidars. It shows in Fig. S1 that CL31 underestimates at low PBL height and overestimates at high PBL height. Thus, the PBL heights derived from the MPL are used in the following part of this paper. The PBL heights in pollution condition varies from 150 m to 1000 m and the heights under 500 m accounts for 87 %.

The PBL heights retrieved by measuring the attenuated backscatter profile of MPL and CL31 still exist some uncertainties (Tang et al.,2016; Geiß et al., 2017). Tang et al. (2016) found that PBL height cannot be correctly obtained through sudden changes in the attenuated backscatter profiles. Such as in situation that the strong northerly winds with dry and clear air masses

32

prevail in observation site, the atmospheric aerosols spread rapidly and became uniform in the vertical direction, the PBL height was substantially underestimated.

The statistical relationship between PM$_{2.5}$ mass concentration and PBL height is investigated and shown in Fig. 3. It shows that the PM$_{2.5}$ concentration has inversely linear correlation with the PBL height with the R^2 of 0.34 for haze events and negative exponential correlation with the R^2 of 0.48 for fog–haze mixed events, indicating that the PM$_{2.5}$ concentration is more sensitive to the PBL height in fog–haze mixed events. The PM$_{2.5}$ concentrations of 50 µg m^{-3}, 100 µg m^{-3}, 200 µg m^{-3}, 300 µg m^{-3}, and 400 µg m^{-3}, correspond to the PBL heights of 830 m, 510 m, 330 m, 300 m, and 290 m, respectively in fog–haze mixed events. The PM$_{2.5}$ concentrations of 100 µg m^{-3}, 200 µg m^{-3}, 300 µg m^{-3} correspond to the PBL heights of 460 m, 370 m and 280 m, respectively, in the haze events. When using CL31 data, we find that the basic relationship can be the same as that by using data from MPL, however, the correlation coefficients decrease substantially. The figure S2 shows that the PM$_{2.5}$ concentration has inversely linear correlation with the PBL height with the R^2 of 0.2 for haze events and negative exponential correlation with the R^2 of 0.34 for fog–haze mixed events. R^2 are both lower than that determined by MPL.

The feedback between PBL height and PM$_{2.5}$ mass concentration is obviously different in the haze events and fog–haze mixed events. In the haze events the PM$_{2.5}$ mass concentration increases almost linearly with the decrease of PBL height, while in the fog–haze mixed events the PM$_{2.5}$ mass concentration initially tends to show a relatively slow increase with the decrease of PBL height. As long as the PBL decreases to the height below 400–500 m, the slight decrease of PBL height could cause a rapid increase of PM$_{2.5}$ mass concentration. Petäjä et al. (2016) investigated the haze cases in Nanjing city and pointed out that the aerosol–boundary layer feedback remained moderate at fine particulate matter concentrations lower than about 200 µg m^{-3}, but that it became increasingly effective at higher particulate matter loadings. Our investigation shows that this phenomenon becomes more obvious in fog–haze mixed event.

3.3 Relationship between visibility and PBL height

Theoretically, the relationship between PBL height and atmospheric visibility is not obvious under clean and clear condition. However, under polluted conditions the variation of PBL height may directly cause the variation of aerosol concentration within the PBL, and induce the change of visibility. The statistical results in Fig. 4 show that there are strong relationships between visibility and PBL height for both haze and fog–haze mixed events. A positive linear correlation with the R^2 of 0.35 exists in haze events and positive exponential correlation with the R^2 of 0.56 exists in fog–haze mixed events between visibility and PBL height.

3.4 Physical mechanism responsible for the relationship among PM$_{2.5}$, visibility and PBL height

To clarify the physical mechanism responsible for the relationship among PM$_{2.5}$, visibility and PBL height obtained above, two typical cases of long-lasting haze and fog–haze mixed events are presented and further investigated in considering their representativeness and data completeness of all cases (Table 1). In all haze events, the haze event observed from 11 to 14 April was highly polluted with the maximum PM$_{2.5}$ concentration of 304 µg m^{-3} and minimum visibility of 1113 m. For all fog–haze

mixed events, the fog duration was considered firstly. Two cases are chosen, in which the fog duration accounted for more than 40 % of the total. One was observed from 19 to 26 February 2014, and the other was occurred from 6 to 11 October 2014. The maximum $PM_{2.5}$ concentration was more higher and the maximum RH reached to 100% in the fog–haze event occurred from 6 to 11 October 2014, which was chosen as typical fog–haze event for the following study.

5 **3.4.1 Typical haze event**

A typical haze event in April 2014 lasting for 74 hours starting at 22:00 LST (Local Standard Time) on 11 April and ending at 23:00 on 14 April during which visibility was less than 10000 m. The synoptic situation during the haze event characterized as a saddle field. Beijing was located in a saddle between two pairs of high and low pressure center. This weather system would lead to calm surface wind and stably stratified atmospheric condition, which was favourable for the accumulation of air 10 pollutants. A cold front passed through Beijing on April 14 and ended the long–lasting haze event.

Figure 5 shows the temporal variations of surface meteorological and environmental factors in the whole process of the haze event. Both air temperature and RH presented a clear diurnal cycle, but they showed a gradually increasing tendency during the haze period due to the persistent southwest warm and humid airflow. The temperature increased from 7.9 ℃ to 25 ℃, with an average of 16.6±5.1 ℃, while the RH was in the range of 28 % to 89 %, with an average of 55±17 %. The variation of RH 15 inversely corresponded that of temperature. The temperature and RH derived from PMWR showed a consistent tendency with those observed by surface automatic weather station. The wind speed varied from 0 m s^{-1} to 3.9 m s^{-1}, with an average of 0.8 m s^{-1}, suggesting that the horizontal diffusion of aerosols was very weak. The $PM_{2.5}$ mass concentration was inversely correlated with visibility. $PM_{2.5}$ reached the highest at 12:00 on 14 April with the value of 304 µg m^{-3}, corresponding to the hourly mean visibility of 1317 m. $PM_{2.5}$ decreased dramatically after 21:00 on 14 April. The visibility continued to rise until 20 the end of the event. The average $PM_{2.5}/PM_{10}$ is as high as 0.82, implying that fine particles were dominant in the atmosphere. The temporal variation of vertical distributions of temperature, RH, LWC and vapor density retrieved by MWRP during the whole haze event is shown in Fig. 6. Many studies demonstrated that PMWR is a useful tool to sense the thermodynamic structure of the lower troposphere continuously by providing profiles of temperature and humidity with reasonable accuracy and height resolution (Ware et al., 2003, 2013; Xu et al., 2015). The inter–comparison with the radiosonde data demonstrated 25 the good correlation of temperature and vapor density retrievals (Guo and Guo, 2015; Xu et al., 2015). The biases of temperature retrieved by PMWR against radiosondes increased with height, and the maximum of bias is 4 ℃ under 2000 m; the bias of water vapor profile was smaller than 1 g m^{-3} (Guo and Guo, 2015). Compared to the radiosonde temperature profiles in Fig. 9a, c, due to the lower vertical resolution, the PMWR could not capture the temperature inversions at the upper level. But the relatively high RH value could be well captured at the height between 700 m to 1600 m, indicating the dominant south– 30 westerly warm and humid airflow during the haze event. The LWC was less than 0.01g m^{-3}.

Figure 7 shows the time–height distribution of the backscatter density detected by the CL31 and the normalized relative backscatter (NRB) of MPL, and time evolutions of the MPL–derived PBL height and $PM_{2.5}$ mass concentration during the

34

删除的内容: 10 km

删除的内容: col pressure field covering North China Plain

删除的内容: 6

删除的内容: microwave radiometer

删除的内容: transport

删除的内容: 7

删除的内容: ; Ware et al.

删除的内容: 2 km

删除的内容: 10 (a) and (c)

删除的内容: 0.7 km

删除的内容: 1.6 km

删除的内容: -

删除的内容: 8

whole haze event. Compared to the MPL, CL31 could not detect all backscatter of the haze aerosols in fine particles due to the longer lidar wavelength (910 nm). Figure 7b shows that the height indicated by the high value of NRB tended to decrease during the whole haze event, indicating that the PBL height tended to decrease with time evolution until in the end of the haze event. Generally, a negative correlation or negative feedback can be found between $PM_{2.5}$ concentration and PBL height (Fig.

5 7c). However, the feedback between $PM_{2.5}$ concentration and PBL height was relatively weak when the $PM_{2.5}$ concentration was below 200 µg m^{-3}. When $PM_{2.5}$ concentration was above 200 µg m^{-3}, the negative feedback became strong. For example, before 14 April, the daily averaged PBL height was above 400 m and the $PM_{2.5}$ concentration was generally below 200 µg m^{-3}. After 14 April, the PBL height rapidly reduced to 300 m and then the $PM_{2.5}$ concentration increased its maximum value of 300 µg m^{-3}. The interesting phenomenon has similar result recently obtained in Nanjing city in south China (Petäjä et al.,

10 2016). The lowing PBL height compressed the aerosol particles into a shallow vertical layer, and prevented the vertical dispersion of the aerosol particles, leading to an increase in the surface aerosol concentrations, which is consistent to the previous study in the region (Quan et al., 2014).

To reveal the lowing process of the PBL height, the time–pressure distribution of vertical velocities in Beijing from 11 to 14 April 2014 is presented in Fig. 8. It indicates that before 13 April, the atmospheric layer from the surface to the middle of

15 troposphere was under a weak updraft condition that was favoured the upward diffusion of aerosols. After 13 April, the downdraft zone started to develop at the upper levels of boundary layer. The formation of this downdraft zone strongly suppressed the upward diffusion of polluted aerosol particles. The PBL height would be lowed, which forced the $PM_{2.5}$ to concentrate at the lower layers and further deteriorated air quality. Therefore, the occurrence of the downdraft zone was one of the important factors to decrease PBL height during the haze event.

20 The aerosol–boundary layer feedback by blocking solar radiation process was suggested as a plausible explanation for the most severe haze episodes in the regions of China (Ding et al., 2016; Petäjä et al., 2016). However, the mechanism that causes the formation of downdraft zone has not been fully understood due to lack of the direct observational data. Since the formation of the downdraft zone can be caused by many mechanisms such as a cooling process induced by upper–level cold air intrusion or cloud process, or an enhanced long–wave radiation emission at the top of boundary layer due to the high accumulation of

25 aerosols at this level. In the daytime, the growth of the PBL height is strongly depended on the surface solar radiation. In the clear day, the PBL can be fully developed through the solar radiation heating. However, if solar radiation is absorbed or scattered by aerosol particles or clouds, the PBL cannot be fully developed, and the daytime PBL heights can be significantly reduced (Yu et al., 2002).

Table 3 presents the parameters of radiation from Beijing Meteorological station during the haze event. It shows that the daily

30 total horizontal plane direct radiation was significantly reduced from 7.67 MJ m^{-2} d^{-1} on 13 April to 4.91 MJ m^{-2} d^{-1} on 14 April, and at the same time the amount of total scattering radiation was increased from 11.07 MJ m^{-2} d^{-1} to 12.65 MJ m^{-2} d^{-1}. These results demonstrate that aerosol particles played important roles for reducing the solar radiation and inhibited the development of PBL heights during the daytime haze event.

To investigate the influence of surface radiation change on temperature profile and characteristic of temperature and humidity variations in the whole haze event, the profiles of temperature and RH are displayed in Fig. 9. The apparent features of vertical temperature and RH profiles were the formation of double inversion layers during the whole haze event. The formation of the upper–level inversion layer at around 1200–1600 m should be closely associated with the advection of southwest warm and humid air. Temperature, RH and wind distribution in 925 and 850 hPa at 08:00 BST on 13 April 2014 are shown in Fig. S3, from which we could see the weak warm advection from the southwest and west at 925 hPa and 850 hPa, respectively. Relatively high RH values were also observed at the height between 700 m and 1600 m in Fig. 6b. The nighttime low–level inversion layer below 150 m should be formed by surface longwave radiation cooling while the formation of the daytime low–level inversion layer at around 150–600 m was complex and hard to explain with simple factors. The temperature profiles in the daytime in Fig. 9a show that a shallow and weak inversion layer was initially formed at 08:00 on 12 April. And then a deep inversion layer slightly above the surface was formed on 13 April and further developed on 14 April. The air cooling at the low–level inversion top where aerosols accumulated was obvious from 13–14 April. However, the formation of a deep inversion layer from 150–600 m was hard to explain by cooling process of aerosol loadings. It is obvious that with the increased accumulation of polluted aerosols in the daytime the low–level stable layer height was increased and its stability was further strengthened. For example, the inversion layer from 150 m to 550 m with the lapse rate of air temperature is −0.38 ℃ (100 m)$^{-1}$ at 8:00 on 13 April, while the lapse rate of the same layer is −0.75 ℃ (100 m)$^{-1}$ at the same time on 14 April.

The formation of the deep inversion layer in the daytime has not been well understood. Some researchers suggested that the heating process due to the solar radiation absorption by aerosols such as black carbon might play an important role in forming the deep inversion layer (Ding et al., 2016; Petäjä et al., 2016). This might be true for the formation of the deep low–level inversion layer shown in Fig. 9a, but it is hard to explain the temperature increase in the whole vertical boundary layer and downward movement of air shown in Fig. 8. It seems that the descending of the upper–level inversion layer was critical to increase the temperature and humidity in the whole boundary layer in the daytime based on the changes of their profiles in Fig. 9.

In all, the persistent advection of southwest warm and humid air provided a long–lasting favourable condition for the formation of a stable upper–level inversion layer of PBL that weakened the upward mixing and diffusing of surface polluted aerosols. As long as the accumulation of aerosols reached certain concentration, the surface cooling induced by the high aerosol loading via blocking the incoming solar radiation became obvious and formed a low–level inversion layer. The formation of the low–level inversion and subsequent further cooling induced a descending process of PBL height and upper–level inversion layer. The descended warm and humid air from the upper inversion layer significantly strengthen the low–level stability and in return rapidly increase the aerosol loadings. The positive feedback was particularly strong when the PM$_{2.5}$ mass concentration was larger than 150–200 μg m^{-3}. Therefore, the descended upper–level inversion layer should be an important factor in strengthening the stability in the whole PBL.

删除的内容: 10

删除的内容: 11

删除的内容: 0.7 km

删除的内容: 1.6 km

删除的内容: 7 (b)

删除的内容: 10 (a)

删除的内容: 10

删除的内容: 9

删除的内容: 10

3.4.2 Typical fog–haze mixed event

The typical fog–haze mixed event started at 22:00 on 6 October and ended at 18:00 on 11 October 2014 with duration of 117 h. During the whole period, the North China Plain was controlled by the westerly airflow in the mid–troposphere. At the surface, a weak pressure field maintained before the arrival of the cold front, with light winds and high humidity. Moreover, the drizzle rain occurred in Beijing in the morning of 8 October, which further increased the atmospheric humidity in the PBL. The radiation fogs formed from 9 to 11 October. The fog lasted 48 hours in total and accounted for 42 % of the duration of the fog–haze mixed event.

Figure 10 shows the temporal evolution of surface meteorological and environmental factors in the whole process of the fog–haze mixed event. During the fog–haze mixed events, wind speed varied from 0 m s^{-1} to 2.7 m s^{-1}, with an average of 0.5 m s^{-1}. The wind direction was easterly from the midnight to afternoon and then changed to calm wind until the next day morning. The temperature was in the range of 9.1 ℃ to 21.7 ℃, with an average of 15.6±3.1 ℃, while the RH was in the range of 46 % to 100 %, with an average of 88±14 %. The visibility exponentially decreased with the PM$_{2.5}$ mass concentration increasing with the R^2 of 0.87. The visibility decreased to the minimum 534 m in the morning of 11 October. PM$_{2.5}$ reached the highest at 19:00 on 9 October with the value of 392 µg m^{-3}, corresponding to the hourly mean visibility of 898 m. After that there was a slight invasion of cold air, PM$_{2.5}$ concentration decreased but still in high level. The decreasing of the temperature was favourable to the formation of fog. PM$_{2.5}$ decreased dramatically after 17:00 on 11 October. The visibility continued to rise until the end of the event. The averaged PM$_{2.5}$/PM$_{10}$ was as high as 0.94.

The temporal variation of vertical distributions of temperature, RH, LWC and vapor density retrieved by MWRP during the whole fog–haze mixed event is shown in Fig. 11. When the precipitation events happened in the morning of 8 October, the profiles became unreliable due to contamination of rainwater on the sensor covering. The LWC was larger than 0.02 g m^{-3} in the morning of 10 and 11 October, which also indicated the fog formation (Guo and Guo, 2015). Moreover, the RH was high near the surface in the morning from 8 to 11 October. Relatively high RH values were also observed at the height between 500 m to 1600 m. Compared to the radiosonde temperature profiles in Fig. 14a, c, the PMWR could not capture the temperature inversions at the upper level. Compared with the haze event, the fog–haze mixed event had a higher RH and induced the fog and drizzle formation, so the surface cooling induced by blocking the incoming solar radiation and subsequent descending process of PBL height became more obvious.

Figure 12 shows the time–height distribution series of the backscatter density detected by CL31 and the NRB detected by MPL, and time evolution of the MPL–derived PBL height and PM$_{2.5}$ mass concentration during the whole fog–haze mixed event. As seen in the Fig. 12a, b, aerosols were mostly confined to a shallow layer of few hundred meters. Due to the longer lidar wavelength, the CL31 has better detection capability of the raindrop and fog droplets compared to the MPL. Comparing with the haze event, the fog and rain drops had stronger attenuation to the signal of MPL. So that the period 1 and 2 in the Fig. 12b were caused by drizzles, and in the period 3, 4 and 5, the strong attenuation was caused by fog droplets occurred in the high RH conditions. The daily averaged PBL heights from 7 to 11 October were 660, 350, 270, 270 and 270 m, respectively, while

the daily averaged PM$_{2.5}$ concentrations were 122.7, 249.7, 333.3, 310.8, and 235.4 μg m^{-3}, respectively, indicating that the PM$_{2.5}$ concentration increased with the decease of PBL height. Figure 12c showed that the feedback between the PM$_{2.5}$ concentration and PBL height was much stronger in the fog–haze mixed event than that in haze event. It is obvious that the negative feedback between the PM$_{2.5}$ concentration and PBL height was much weak when the PM$_{2.5}$ concentration was less

5 than 200 μg m^{-3}, and it became much strong when the PM$_{2.5}$ concentration reached more than 200 μg m^{-3}.

The time–pressure distribution of vertical velocities during the fog–haze event in Beijing from 6 to 11 October 2014 is presented in Fig. 13. Similar to the haze event in Sect. 3.4.1, the downdraft zone started to form at the upper levels of boundary layer in the afternoon 7 October, and lasted until a cold frontal system passed the area. The downdraft zone decreased from 700 to 850 hPa in the afternoon 7 October, which led to the sharply decrease of PBL height in Fig. 12c. In 9 October, the

10 height of downdraft zone was the lowest and the updraft speed in the PBL was the smallest, corresponding to the most polluted day during the whole fog–haze mixed event.

The surface decrease of radiation parameters was more obvious in the fog–haze mixed event shown in Table 4. Daily total horizontal (vertical) plane direct radiation was significantly reduced from14.11 (24.94) to 0.86 (1.4) MJ m^{-2} d^{-1} during 6–11 October 2014, while the total scattering radiation was increased from 3.4 to 7.21 MJ m^{-2} d^{-1}. These decreases are consistent

15 with the high PM$_{2.5}$ concentration recorded.

Similar to the haze event, the temperature and RH profiles of the fog–haze mixed event also had stronger double inversion layers (Fig. 14). The obvious upper inversion layer was closely associated with strong advection of warm and humid airflow from southwest (Fig. S4). Relatively high RH values were also observed at the height between 500 m to 1700 m in Fig. 11b. The low–level inversion layer from the surface to 300 m in the daytime had the lapse rate of −1.4 ℃ (100 m)$^{-1}$ at 8:00 on 9

20 October. The daily averaged PBL height reached the minimum of 270 m, and lasted until the end of the fog–haze mixed event in the evening 11 October. As discussed above, the stronger daytime low–level inversion in the fog–haze mixed event should be related to the higher aerosol concentration accumulated in the low–level. The higher aerosol concentration caused an obvious decrease of surface solar radiation and surface temperature, meanwhile, the absorption of light–absorbing particles such as black carbon increases the temperature above the surface. These processes formed the stronger low–level temperature

25 inversion during the fog–haze mixed event and induced a more stable PBL. The previous studies showed that the black carbon could contribute a fraction of about 3–15 % to the total mass concentrations in urban air (Yang et al., 2011; Huang et al., 2014). A total of 476 fires caused by biomass burning were observed by MODIS of Terra (10:30) and Aqua (13:30) during the fog–haze mixed event in China according to the Ministry of Environment Protection of the People's Republic of China (http://www.zhb.gov.cn/hjzl/dqhj/jgjsjcbg/). The nighttime low–level inversion layer was relatively weaker in the fog–haze

30 mixed event than that in the haze event. This is because that the surface long–wave radiation cooling may rapidly cause the formation of fog as long as the air saturation condition is reached. When the fog is formed, the released latent heating in fog formation will heat the air and weaken the inversion structure.

Table 5 summarizes the averaged PM$_{2.5}$ mass concentration, PBL height, RH and radiation parameters in the haze and fog–haze mixed event. The averaged PM$_{2.5}$ concentration was 164.5 and 250.4 μg m^{-3} in the haze event and fog–haze mixed event,

删除的内容: 14 (c)

删除的内容: 15

删除的内容: 14 (c)

删除的内容: 16

删除的内容: 17

删除的内容: 0.5 km

删除的内容: 1.7 km

删除的内容: 13 (b)

删除的内容: 0.27 km

respectively. The difference between surface solar radiations of the haze event and fog–haze mixed event was mainly due to the column accumulation of aerosol and fog drops extinction. Compared with the haze event, the reduction of the surface solar total radiation was 8.88 MJ m^{-2} in the fog–haze mixed event. The total horizontal plane direct radiation and vertical plane direct radiation decreased 4.9 and 5.95 MJ m^{-2}, respectively. The average of total scattering radiation rate (the radio of total scattering radiation and total radiation) increased by 17 %. The radiation reduction imposed by aerosol particles was particularly stronger during the fog–haze mixed event. Solar radiation absorbed by the surface of the Earth, heats the bottom of atmospheric column producing convective eddies that transport heat and water vapor upward driving the growth of the PBL (Lee and Ngan, 2011). So, the daily averaged PBL height was lower by 110 m in the fog–haze mixed event.

We proposed that the PBL feedback is much stronger in fog–haze mixed event than in haze event. This is because that the fog–haze events included many fog droplets, which can substantially block the solar radiation comparing with aerosol loading in haze events in the daytime and cause stronger surface cooling. The stronger surface cooling would cause stronger descending of the upper inversion layer and then form a highly suppressed and more stable PBL. So the PBL feedback was much stronger in fog-haze event. As seen in Table 5, the radiation reduction imposed by aerosol particles was particularly stronger during the fog–haze mixed event than the haze event. The PM$_{2.5}$ concentration is higher and the PBL heights are lower in the fog–haze mixed event.

4 Conclusion and discussions

In this study, the relationship among PBL height, PM$_{2.5}$ mass concentration and visibility for long–lasting haze and fog–haze mixed events in Beijing was investigated and quantified. Comprehensive measurements of aerosol characteristics and meteorological conditions have been conducted in Chinese Academy of Meteorological Sciences (CAMS), Beijing since 2013, and a total of 11 long–lasting haze and fog–haze mixed events were observed from January 2014 to March 2015. PBL heights of haze and fog–haze mixed events were retrieved using MPL NRB signal and well correlated to the PBL height derived by CL31.

The statistical results show that there was a negative exponential function between the visibility and the PM$_{2.5}$ mass concentration for both haze and fog–haze mixed events with the same R^2 of 0.80. Aerosols could cause greater visibility impairments in fog–haze mixed events due to the increase of RH and formation of more fog drops.

The PM$_{2.5}$ concentration had inversely linear correlation with PBL height for haze events with the R^2 of 0.34 and negative exponential correlation with the R^2 of 0.48 for fog–haze mixed events, indicating that the PM$_{2.5}$ concentration is more sensitive to PBL height in fog–haze mixed events. The feedback between PBL height and PM$_{2.5}$ mass concentration became stronger when PM$_{2.5}$ mass concentration was more than 150–200 µg m^{-3}, particularly in fog–haze mixed cases, which is similar to the finding in haze events in Nanjing city (Petäjä et al., 2016). However, our investigation shows that this phenomenon became more obvious in the fog–haze mixed event.

删除的内容: 0.11 km

删除的内容: 49

Similarity to the relationship between $PM_{2.5}$ concentration and PBL height, a positive linear correlation with the R^2 of 0.35 existed in haze events and positive exponential correlation with the R^2 of 0.56 existed in fog–haze mixed events between visibility and PBL height.

Two typical cases representing for haze and fog–haze mixed events are presented and discussed. The main results show the
5 obvious double inversion layers located at upper–level and low–level respectively formed in both cases. The formation of upper–level inversion layer was closely associated with the persistent advection of southwest warm and humid air. The nighttime low–level inversion layer was formed due to the surface longwave radiation cooling, while the formation of daytime low–level inversion layer was complex. Our study shows that the initial daytime low–level inversion layer should be related to the surface cooling via blocking the incoming solar radiation by high aerosol loadings. The subsequent rapid development
10 of deep low–level inversion layer in the daytime is hard to explain only by the surface cooling process. We suggest that both the heating process due to the solar radiation absorption by accumulated aerosols such as black carbon and the descended upper–level warm and humid air induced by the surface cooling played critical role in the daytime. Since the strong surface cooling could collapse PBL and cause an obviously lowing PBL height, and this process could also cause the warm and humid air at upper inversion layer to move downward and induced an increase of temperature and humidity at low air levels. The
15 process can be clearly shown in the case of this study and it might be an important factor in strengthening low–level stability in the daytime. The positive feedback was particularly strong when the $PM_{2.5}$ mass concentration was larger than 150–200 μg m^{-3}. Therefore, the descended upper–level inversion layer should be an important factor in strengthening the stability in the whole PBL.

The main differences of meteorological condition for two cases are humidity and duration. Although both cases occurred in a
20 stable weak pressure field covering northern China, the haze event was drier and duration was shorter while the fog–haze mixed event was more humid and had a longer duration. Since the fog droplets were formed in the fog–haze mixed event, the radiation reduction at surface was more obvious and stronger, and caused stronger descending process of the upper inversion layer. In most cases, light precipitation (drizzle rain or light snow) occurred during the fog–haze mixed event while in all haze events during the observation period, there was no precipitation. The fog–haze mixed event was more favorable to form
25 extremely high mass concentration of $PM_{2.5}$ (>300 μg m^{-3}) than the haze event.

The new finding in this paper has important implications in explaining the frequent long–lasting polluted events in the study region. Generally, a typical pollution event is usually formed under a stable and shallow temperature–inversion condition at low atmospheric layers, and would disappear or obviously decrease when the daytime solar radiation increases. However, in the study region, we found that many severe haze and fog–haze mixed events lasted for several days even for several weeks.
30 Most previous publications attributed the reason as the persistent abnormal weather system or high emissions. However, this study shows that except for the influence of meteorological condition and high emission, the interactions and feedbacks between PBL and aerosol loading linked by radiation process are crucial in enhancing and maintaining these polluted events. These feedbacks could cause an important variation of dynamical/thermal processes in lower troposphere. The formation of double inversion layer and their subsequent change is closely associated with persistent meteorological condition, high aerosol

loading and associated radiation process. Due to the complex interactions and feedbacks, a deeper and more stable atmospheric low–level is formed and it is hard to break up by daytime solar radiation heating process until the strong wind occurs and removes the high aerosol loading.

Competing interests

5   The authors declare they have no conflict of interest.

10   **References**

Andreae, M. O., and Rosenfeld, D.: Aerosol–cloud–precipitation interactions. Part 1. The nature and sources of cloud–active aerosols, Earth Sci. Rev., 89, 13–41, doi:10.1016/j.earscirev.2008.03.001, 2008.

Baumer, D., Vogel, B., Versick, S., Rinke, R., Mohler, O., and Schnaiter, M.: Relationship of visibility, aerosol optical thickness and aerosol size distribution in an ageing air mass over South–West Germany, Atmos. Environ., 42, 989–998, 15   doi:10.1016/j.atmosenv.2007.10.017, 2008.

Boyouk, N., Léon, J. F., Delbarre, H., Podvin, T., and Deroo, C.: Impact of the mixing boundary layer on the relationship between $PM_{2.5}$ and aerosol optical thickness, Atmos. Environ., 44, 271–277, doi:10.1016/j.atmosenv.2009.06.053, 2010.

Brooks, I. M.: Finding Boundary Layer Top: Application of a Wavelet Covariance Transform to Lidar Backscatter Profiles, J. Atmos. Ocean. Tech., 20, 1092–1105, doi:10.1175/1520-0426(2003)020<1092:fbltao>2.0.co;2, 2003.

20   Cai, W., Li, K., Liao, H., Wang, H., and Wu, L.: Weather conditions conducive to Beijing severe haze more frequent under climate change, Nature Clim. Change, 7, 257-262, doi:10.1038/nclimate3249, 2017.

Campbell, J. R., Hlavka, D. L., Welton, E. J., Flynn, C. J., Turner, D. D., Spinhirne, J. D., Scott, V. S., and Hwang, I. H.: Full–time, eye–safe cloud and aerosol lidar observation at atmospheric radiation measurement program sites: Instruments and data processing, J. Atmos. Ocean. Tech., 19, 431–442, doi:10.1175/1520-0426(2002)019<0431:ftesca>2.0.co;2, 2002.

25   Campbell, J. R., Sassen, K., and Welton, E. J.: Elevated Cloud and Aerosol Layer Retrievals from Micropulse Lidar Signal Profiles, J. Atmos. Ocean. Tech., 25, 685–700, doi:10.1175/2007jtecha1034.1, 2008.

Cao, J. J., Wang, Q. Y., Chow, J. C., Watson, J. G., Tie, X. X., Shen, Z. X., Wang, P., and An, Z. S.: Impacts of aerosol compositions on visibility impairment in Xi'an, China, Atmos. Environ., 59, 559–566, doi:10.1016/j.atmosenv.2012.05.036, 2012.

Chan, C. K., and Yao, X. H.: Air pollution in mega cities in China, Atmos. Environ., 42, 1–42, doi:10.1016/j.atmosenv.2007.09.003, 2008.

Chen, H., and Wang, H.: Haze Days in North China and the associated atmospheric circulations based on daily visibility data from 1960 to 2012, J. Geophys. Res. Atmos., 120, 5895-5909, 10.1002/2015JD023225, 2015.

5 Chen, J., Zhao, C. S., Ma, N., Liu, P. F., Gobel, T., Hallbauer, E., Deng, Z. Z., Ran, L., Xu, W. Y., Liang, Z., Liu, H. J., Yan, P., Zhou, X. J., and Wiedensohler, A.: A parameterization of low visibilities for hazy days in the North China Plain, Atmos. Chem. Phys., 12, 4935–4950, doi:10.5194/acp-12-4935-2012, 2012.

Chen, R. J., Zhao, Z. H., and Kan, H. D.: Heavy Smog and Hospital Visits in Beijing, China, Am. J. Respir. Crit. Care. Med., 188, 1170–1171, doi:10.1164/rccm.201304-0678LE, 2013.

10 Chen, W. B., Kuze, H., Uchiyama, A., Suzuki, Y., and Takeuchi, N.: One–year observation of urban mixed layer characteristics at Tsukuba, Japan using a micro pulse lidar, Atmos. Environ., 35, 4273–4280, doi:10.1016/s1352-2310(01)00181-9, 2001.

Cho, Y. K., Kim, M. O., and Kim, B. C.: Sea fog around the Korean peninsula, J. Appl. Meteorol., 39, 2473-2479, doi:10.1175/1520-0450(2000)039<2473:sfatkp>2.0.co;2, 2000.

Chou, C. C. K., Lee, C. T., Chen, W. N., Chang, S. Y., Chen, T. K., Lin, C. Y., and Chen, J. P.: Lidar observations of the 15 diurnal variations in the depth of urban mixing layer: a case study on the air quality deterioration in Taipei, Taiwan, Sci. Total Environ., 374, 156–166, doi:10.1016/j.scitotenv.2006.11.049, 2007.

Cimini, D., Campos, E., Ware, R., Albers, S., Giuliani, G., Oreamuno, J., Joe, P., Koch, S. E., Cober, S., and Westwater, E.: Thermodynamic Atmospheric Profiling During the 2010 Winter Olympics Using Ground-Based Microwave Radiometry, IEEE Trans. Geosci. Remote Sens., 49, 4959–4969, doi:10.1109/tgrs.2011.2154337, 2011.

20 Di, Q., Wang, Y., Zanobetti, A., Wang, Y., Koutrakis, P., Choirat, C., Dominici, F., and Schwartz, J. D.: Air Pollution and Mortality in the Medicare Population, N. Engl. J. Med., 376, 2513-2522, doi:10.1056/NEJMoa1702747, 2017.

Ding, A. J., Huang, X., Nie, W., Sun, J. N., Kerminen, V. M., Petaja, T., Su, H., Cheng, Y. F., Yang, X. Q., Wang, M. H., Chi, X. G., Wang, J. P., Virkkula, A., Guo, W. D., Yuan, J., Wang, S. Y., Zhang, R. J., Wu, Y. F., Song, Y., Zhu, T., Zilitinkevich, S., Kulmala, M., and Fu, C. B.: Enhanced haze pollution by black carbon in megacities in China, Geophys. Res. Lett., 43, 25 2873–2879, doi:10.1002/2016gl067745, 2016.

Elias, T., Haeffelin, M., Drobinski, P., Gomes, L., Rangognio, J., Bergot, T., Chazette, P., Raut, J. C., and Colomb, M.: Particulate contribution to extinction of visible radiation: Pollution, haze, and fog, Atmos. Res., 92, 443–454, doi:10.1016/j.atmosres.2009.01.006, 2009.

Eresmaa, N., Karppinen, A., Joffre, S. M., Räsänen, J., and Talvitie, H.: Mixing height determination by ceilometer, Atmos. 30 Chem. Phys., 6, 1485–1493, doi:10.5194/acp-6-1485-2006, 2006.

Eresmaa, N., Härkönen, J., Joffre, S. M., Schultz, D. M., Karppinen, A., and Kukkonen, J.: A Three-Step Method for Estimating the Mixing Height Using Ceilometer Data from the Helsinki Testbed, Jappl. Meteorol. Clim., 51, 2172–2187, doi:10.1175/jamc-d-12-058.1, 2012.

Fernald, F. G.: Analysis of atmospheric lidar observations: some comments, Appl. Opt., 23, 652–653, 35 doi:10.1364/AO.23.000652, 1984.

Gao, H., and Li, X.: Influences of El Nino Southern Oscillation events on haze frequency in eastern China during boreal winters, Int. J. Climatol. , 35, 2682-2688, doi:10.1002/joc.4133, 2015.

Gao, Y., Zhang, M., Liu, Z., Wang, L., Wang, P., Xia, X., Tao, M., and Zhu, L.: Modeling the feedback between aerosol and meteorological variables in the atmospheric boundary layer during a severe fog-haze event over the North China Plain, Atmos.
5   Chem. Phys., 15, 4279–4295, doi:10.5194/acp-15-4279-2015, 2015.

Geiß, A., Wiegner, M., Bonn, B., Schäfer, K., Forkel, R., von Schneidemesser, E., Münkel, C., Chan, K. L., and Nothard, R.: Mixing layer height as an indicator for urban air quality?, Atmos. Meas. Tech., 10, 2969-2988, doi:10.5194/amt-10-2969-2017, 2017.

Gultepe, I., Zhou, B., Milbrandt, J., Bott, A., Li, Y., Heymsfield, A. J., Ferrier, B., Ware, R., Pavolonis, M., Kuhn, T., Gurka,
10 J., Liu, P., and Cermak, J.: A review on ice fog measurements and modeling, Atmos. Res., 151, 2–19, doi:10.1016/j.atmosres.2014.04.014, 2015.

Guo, L. J., and Guo, X. L.: Verification study of the atmospheric temperature and humidity profiles retrieved from the ground–based multi–channels microwave radiometer for persistent foggy weather events in northern China, Acta Meteorologica Sinica, 73, 368–381, doi: 10.11676/qxxb2015.025, 2015. (in Chinese)

15 Guo, L., Guo, X., Fang, C., and Zhu, S.: Observation analysis on characteristics of formation, evolution and transition of a long-lasting severe fog and haze episode in North China, Sci. China Earth Sci., 58, 329–344, doi: 10.1007/s11430-014-4924-2, 2015.

Haeffelin, M., Angelini, F., Morille, Y., Martucci, G., Frey, S., Gobbi, G. P., Lolli, S., O'Dowd, C. D., Sauvage, L., Xueref-Rémy, I., Wastine, B., and Feist, D. G.: Evaluation of mixing–height retrievals from automatic profiling lidars and ceilometers
20 in view of future integrated networks in Europe, Bound.-Lay. Meteorol., 143, 49–75, doi:10.1007/s10546-011-9643-z, 2012.

Han, L., Zhou, W., and Li, W.: Fine particulate ($PM_{2.5}$) dynamics during rapid urbanization in Beijing, 1973–2013, Sci. Rep., 6, doi:10.1038/srep23604, 2016.

Han, X., Zhang, M. G., Tao, J. H., Wang, L. L., Gao, J., Wang, S. L., and Chai, F. H.: Modeling aerosol impacts on atmospheric visibility in Beijing with RAMS-CMAQ, Atmos. Environ., 72, 177–191, doi:10.1016/j.atmosenv.2013.02.030, 2013.

25 He, Q. S., Li, C. C., Mao, J. T., Lau, A. K. H., and Chu, D. A.: Analysis of aerosol vertical distribution and variability in Hong Kong, J. Geophys. Res., 113, doi:10.1029/2008JD009778, 2008.

Huang, R. J., Zhang, Y. L., Bozzetti, C., Ho, K. F., Cao, J. J., Han, Y. M., Daellenbach, K. R., Slowik, J. G., Platt, S. M., and Francesco, C.: High secondary aerosol contribution to particulate pollution during haze events in China, Nature, 514, 218–222, doi:10.1038/nature13774, 2014.

30 Kang, H. Q., Zhu, B., Su, J. F., Wang, H. L., Zhang, Q. C., and Wang, F.: Analysis of a long–lasting haze episode in Nanjing, China, Atmos. Res., 120–121, 78–87, doi:10.1016/j.atmosres.2012.08.004, 2013.

Klein, C., and Dabas, A.: Relationship between optical extinction and liquid water content in fogs, Atmos. Meas. Tech., 7, 1277–1287, doi:10.5194/amt-7-1277-2014, 2014.

Köhler, H.: The nucleus in and the growth of hygroscopic droplets, Transactions of the Faraday Society, 32, 1152-1161, doi:
35 10.1039/TF9363201152, 1936.

已移动(插入) [1]

已上移 [1]: Han, L., Zhou, W., and Li, W.: Fine particulate ($PM_{2.5}$) dynamics during rapid urbanization in Beijing, 1973–2013, Sci. Rep., 6, doi:10.1038/srep23604, 2016.

Lee, P., and Ngan, F.: Coupling of Important Physical Processes in the Planetary Boundary Layer between Meteorological and Chemistry Models for Regional to Continental Scale Air Quality Forecasting: An Overview, Atmosphere, 2, 464–483, doi:10.3390/atmos2030464, 2011.

5 Li, Q., Zhang, R. H., and Wang, Y.: Interannual variation of the wintertime fog-haze days across central and eastern China and its relation with East Asian winter monsoon, Int. J. Climatol., 36, 346-354, doi:10.1002/joc.4350, 2016.

Li, Y., Zhao, H. J., and Wu, Y. F.: Characteristics of Particulate Matter during Haze and Fog (Pollution) Episodes over Northeast China, Autumn 2013, Aerosol Air Qual. Res., 15, 853–864, doi:10.4209/aaqr.2014.08.0158, 2015.

Liao, H., Chang, W. Y., and Yang, Y.: Climatic Effects of Air Pollutants over China: A Review, Adv. Atmos. Sci. , 32, 115-139, doi:10.1007/s00376-014-0013-x, 2015.

10 Liu, J., Xia, X., Wang, P., Li, Z., Zheng, Y., Cribb, M., and Chen, H.: Significant aerosol direct radiative effects during a pollution episode in northern China, Geophys. Res. Lett., 34, doi:10.1029/2007GL030953, 2007.

Martucci, G., Milroy, C., and O'Dowd, C. D.: Detection of Cloud–Base Height Using Jenoptik CHM15K and Vaisala CL31 Ceilometers, J. Atmos. Ocean. Tech., 27, 305–318, doi:10.1175/2009jtecha1326.1, 2010.

Morille, Y., Haeffelin, M., Drobinski, P., and Pelon, J.: STRAT: An Automated Algorithm to Retrieve the Vertical Structure of the Atmosphere from Single-Channel Lidar Data, J. Atmos. Ocean. Tech., 24, 761–775, doi:10.1175/jtech2008.1, 2007.

15 Münkel, C.: Mixing height determination with lidar ceilometers-results from Helsinki Testbed, Meteorol. Z., 16, 451–459, doi:10.1127/0941-2948/2007/0221, 2007.

Münkel, C., and Räsänen, J.: New optical concept for commercial lidar ceilometers scanning the boundary layer, Proceedings of SPIE, 5571, 364–374, doi:10.1117/12.565540, 2004.

20 Münkel, C., Eresmaa, N., Räsänen, J., and Karppinen, A.: Retrieval of mixing height and dust concentration with lidar ceilometer, Bound.-Lay. Meteorol., 124, 117–128, doi:10.1007/s10546-006-9103-3, 2007.

NOAA: Surface weather observations and reports. Federal Meteorological Handbook 94 pp, 1995.

Pandis, S. N., Seinfeld, J. H., and Pilinis, C.: Heterogeneous sulfate production in an urban fog, Atmospheric Environment. Part A. General Topics, 26, 2509–2522, doi:10.1016/0960-1686(92)90103-R, 1992.

25 Petäjä, T., Järvi, L., Kerminen, V. M., Ding, A. J., Sun, J. N., Nie, W., Kujansuu, J., Virkkula, A., Yang, X. Q., Fu, C. B., Zilitinkevich, S., and Kulmala, M.: Enhanced air pollution via aerosol–boundary layer feedback in China, Sci. Rep., 6, doi:10.1038/srep18998, 2016.

Pope, C. A., and Dockery, D. W.: Air pollution and life expectancy in China and beyond, Proc. Natl. Acad. Sci. USA, 110, 12861–12862, doi:10.1073/pnas.1310925110, 2013.

30 Pruppacher, H. R., and Klett, J. D.: Microphysics of clouds and precipitation, Kluwer Acad., Norwell, Mass., 1978.

Qian, Y., Kaiser, D. P., Leung, L. R., and Xu, M.: More frequent cloud-free sky and less surface solar radiation in China from 1955 to 2000, Geophys. Res. Lett., 33, doi:10.1029/2005gl024586, 2006.

Quan, J., Zhang, Q., He, H., Liu, J., Huang, M., and Jin, H.: Analysis of the formation of fog and haze in North China Plain (NCP), Atmos. Chem. Phys., 11, 8205–8214, doi:10.5194/acp-11-8205-2011, 2011.

44

已移动(插入) [2]

已上移 [2]: Martucci, G., Milroy, C., and O'Dowd, C. D.: Detection of Cloud–Base Height Using Jenoptik CHM15K and Vaisala CL31 Ceilometers, J. Atmos. Ocean. Tech., 27, 305–318, doi:10.1175/2009jtecha1326.1, 2010.
Morille, Y., Haeffelin, M., Drobinski, P., and Pelon, J.: STRAT: An Automated Algorithm to Retrieve the Vertical Structure of the Atmosphere from Single-Channel Lidar Data, J. Atmos. Ocean. Tech., 24, 761–775, doi:10.1175/jtech2008.1, 2007.

Quan, J., Gao, Y., Zhang, Q., Tie, X., Cao, J., Han, S., Meng, J., Chen, P., and Zhao, D.: Evolution of planetary boundary layer under different weather conditions,and its impact on aerosol concentrations, Particuology, 11, 34–40, doi:10.1016/j.partic.2012.04.005, 2013.

Quan, J., Tie, X., Zhang, Q., Liu, Q., Li, X., Gao, Y., and Zhao, D.: Characteristics of heavy aerosol pollution during the 2012–2013 winter in Beijing, China, Atmos. Environ., 88, 83–89, doi:10.1016/j.atmosenv.2014.01.058, 2014.

Schween, J. H., Hirsikko, A., Löhnert, U., and Crewell, S.: Mixing-layer height retrieval with ceilometer and Doppler lidar: from case studies to long-term assessment, Atmos. Meas. Tech., 7, 3685–3704, doi:10.5194/amt-7-3685-2014, 2014.

Seinfeld, J. H., and Pandis, S. N.: Atmospheric chemistry and physics: from air pollution to climate change, 2nd ed., John Wiley & Sons, 2012.

Shi, Y., Chen, J. M., Hu, D. W., Wang, L., Yang, X., and Wang, X. M.: Airborne submicron particulate (PM_1) pollution in Shanghai, China: Chemical variability, formation/dissociation of associated semi-volatile components and the impacts on visibility, Sci. Total Environ., 473, 199–206, doi:10.1016/j.scitotenv.2013.12.024, 2014.

Sun, Y., Zhuang, G., Tang, A. A., Wang, Y., and An, Z.: Chemical characteristics of $PM_{2.5}$ and PM_{10} in haze-fog episodes in Beijing, Environ. Sci. Technol., 40, 3148-3155, doi:10.1021/es051533g, 2006.

Sun, Y., Song, T., Tang, G., and Wang, Y.: The vertical distribution of $PM_{2.5}$ and boundary–layer structure during summer haze in Beijing, Atmos. Environ., 74, 413–421, doi:10.1016/j.atmosenv.2013.03.011, 2013.

Sun, Y. L., Jiang, Q., Wang, Z. F., Fu, P. Q., Li, J., Yang, T., and Yin, Y.: Investigation of the sources and evolution processes of severe haze pollution in Beijing in January 2013, J. Geophys. Res., 119, 4380–4398, doi:10.1002/2014jd021641, 2014.

Tang, G. Q., Zhang, J. Q., Zhu, X. W., Song, T., Münkel, C., Hu, B., Schäfer, K., Liu, Z. R., Zhang, J. K., Wang, L. L., Xin, J. Y., Suppan, P., and Wang, Y. S.: Mixing layer height and its implications for air pollution over Beijing, China, Atmos. Chem. Phys., 16, 2459–2475, doi:10.5194/acp-16-2459-2016, 2016.

Tardif, R., and Rasmussen, R. M.: Event-based climatology and typology of fog in the New York City region, Jappl. Meteorol. Clim., 46, 1141-1168, doi:10.1175/jam2516.1, 2007.

Thermo Fisher Scientific: TEOM 1405-DF: Dichotomous Ambient Particulate Monitor with FDMS Option, 16 Septemper 2009.

Tie, X., Wu, D., and Brasseur, G.: Lung cancer mortality and exposure to atmospheric aerosol particles in Guangzhou, China, Atmos. Environ., 43, 2375–2377, doi:10.1016/j.atmosenv.2009.01.036, 2009.

Tsaknakis, G., Papayannis, A., Kokkalis, P., Amiridis, V., Kambezidis, H. D., Mamouri, R. E., Georgoussis, G., and Avdikos, G.: Inter–comparison of lidar and ceilometer retrievals for aerosol and Planetary Boundary Layer profiling over Athens, Greece, Atmos. Meas. Tech., 4, 1261–1273, doi:10.5194/amt-4-1261-2011, 2011.

Vaisala Oyj: Vaisala Ceilometer CL31 User's Guide, 2009

Wang, H., Xu, J., Zhang, M., Yang, Y., Shen, X., Wang, Y., Chen, D., and Guo, J.: A study of the meteorological causes of a prolonged and severe haze episode in January 2013 over central–eastern China, Atmos. Environ., 98, 146–157, doi:10.1016/j.atmosenv.2014.08.053, 2014.

删除的内容: a

45

Wang, H. J., Chen, H. P., and Liu, J. P.: Arctic Sea Ice Decline Intensified Haze Pollution in Eastern China, Atmos. Ocean. Sci. Lett., 8, 1-9, doi:10.3878/AOSL20140081, 2015.

Wang, J., Wang, S., Jiang, J., Ding, A., Zheng, M., Zhao, B., Wong, D. C., Zhou, W., Zheng, G., Wang, L., Pleim, J. E., and Hao, J.: Impact of aerosol-meteorology interactions on fine particle pollution during China's severe haze episode in January
5 2013, Environ. Res. Lett., 9, doi:10.1088/1748-9326/9/9/094002, 2014.

Ware, R., Carpenter, R., Guldner, J., Liljegren, J., Nehrkorn, T., Solheim, F., and Vandenberghe, F.: A multichannel radiometric profiler of temperature, humidity, and cloud liquid, Radio Science, 38, doi:10.1029/2002rs002856, 2003.

Ware, R., Cimini, D., Campos, E., Giuliani, G., Albers, S., Nelson, M., Koch, S. E., Joe, P., and Cober, S.: Thermodynamic and liquid profiling during the 2010 Winter Olympics, Atmos. Res., 132, 278–290, doi:10.1016/j.atmosres.2013.05.019, 2013.

10 Welton, E. J., Voss, K. J., Gordon, H. R., Maring, H., Smirnov, A., Holben, B., Schmid, B., Livingston, J. M., Russell, P. B., Durkee, P. A., Formenti, P., and Andreae, M. O.: Ground-based lidar measurements of aerosols during ACE–2: instrument description, results, and comparisons with other ground–based and airborne measurements, Tellus B, 52, 636–651, doi:10.1034/j.1600-0889.2000.00025.x, 2000.

Welton, E. J., Voss, K. J., Quinn, P. K., Flatau, P. J., Markowicz, K., Campbell, J. R., Spinhirne, J. D., Gordon, H. R., and
15 Johnson, J. E.: Measurements of aerosol vertical profiles and optical properties during INDOEX 1999 using micropulse lidars, J. Geophys. Res., 107, doi:10.1029/2000JD000038, 2002.

Wiegner, M., Madonna, F., Binietoglou, I., Forkel, R., Gasteiger, J., Geiß, A., Pappalardo, G., Schäfer, K., and Thomas, W.: What is the benefit of ceilometers for aerosol remote sensing? An answer from EARLINET, Atmos. Meas. Tech., 7, 1979–1997, doi:10.5194/amt-7-1979-2014, 2014.

20 Xu, G. R., Xi, B. K., Zhang, W. G., Cui, C. G., Dong, X. Q., Liu, Y. Y., and Yan, G. P.: Comparison of atmospheric profiles between microwave radiometer retrievals and radiosonde soundings, J. Geophys. Res., 120, 10313–10323, doi:10.1002/2015jd023438, 2015.

Xu, X., Zhao, T., Liu, F., Gong, S. L., Kristovich, D., Lu, C., Guo, Y., Cheng, X., Wang, Y., and Ding, G.: Climate modulation of the Tibetan Plateau on haze in China, Atmos. Chem. Phys., 16, 1365-1375, doi:10.5194/acp-16-1365-2016, 2016.

25 Yan, Q., Hua, D., Wang, Y., Li, S., Gao, F., Zhou, Z., Wang, L., Liu, C., and Zhang, S.: Observations of the boundary layer structure and aerosol properties over Xi'an using an eye-safe Mie scattering Lidar, J. Quant. Spectrosc. Ra., 122, 97–105, doi:10.1016/j.jqsrt.2012.10.026, 2013.

Yang, D. W., Li, C. C., Lau, A. K. H., and Li, Y.: Long–term measurement of daytime atmospheric mixing layer height over Hong Kong, J. Geophys. Res., 118, 2422–2433, doi:10.1002/jgrd.50251, 2013.

30 Yang, F., Tan, J., Zhao, Q., Du, Z., He, K., Ma, Y., Duan, F., Chen, G., and Zhao, Q.: Characteristics of $PM_{2.5}$ speciation in representative megacities and across China, Atmos. Chem. Phys., 11, 5207–5219, doi:10.5194/acp-11-5207-2011, 2011.

Yang, Y., Liao, H., and Lou, S.: Increase in winter haze over eastern China in recent decades: Roles of variations in meteorological parameters and anthropogenic emissions, J. Geophys. Res. Atmos., 121, 13050-13065, doi:10.1002/2016JD025136, 2016.

35 Yang, Y., Russell, L. M., Lou, S., Liao, H., Guo, J., Liu, Y., Singh, B., and Ghan, S. J.: Dust-wind interactions can intensify aerosol pollution over eastern China, Nat. Commun., 8, doi:15333, 10.1038/ncomms15333, 2017a.

删除的内容: b

已移动(插入) [3]

已上移 [3]: Yang, D. W., Li, C. C., Lau, A. K. H., and Li, Y.: Long–term measurement of daytime atmospheric mixing layer height over Hong Kong, J. Geophys. Res., 118, 2422–2433, doi:10.1002/jgrd.50251, 2013.

Yang, Y., Wang, H., Smith, S. J., Ma, P. L., and Rasch, P. J.: Source attribution of black carbon and its direct radiative forcing in China, Atmos. Chem. Phys., 17, 4319-4336, doi:10.5194/acp-17-4319-2017, 2017b.

Yu, H., Liu, S. C., and Dickinson, R. E.: Radiative effects of aerosols on the evolution of the atmospheric boundary layer, J. Geophys. Res., 107, doi:10.1029/2001JD000754, 2002.

5 Zhang, Q., Streets, D. G., Carmichael, G. R., He, K. B., Huo, H., Kannari, A., Klimont, Z., Park, I. S., Reddy, S., Fu, J. S., Chen, D., Duan, L., Lei, Y., Wang, L. T., and Yao, Z. L.: Asian emissions in 2006 for the NASA INTEX−B mission, Atmos. Chem. Phys., 9, 5131–5153, doi:10.5194/acp-9-5131-2009, 2009.

Zhang, Q., Quan, J. N., Tie, X. X., Li, X., Liu, Q., Gao, Y., and Zhao, D. L.: Effects of meteorology and secondary particle formation on visibility during heavy haze events in Beijing, China, Sci. Total Environ., 502, 578-584, 10 doi:10.1016/j.scitotenv.2014.09.079, 2015.

Zhang, R., Jing, J., Tao, J., Hsu, S. C., Wang, G., Cao, J., Lee, C. S. L., Zhu, L., Chen, Z., Zhao, Y., and Shen, Z.: Chemical characterization and source apportionment of PM$_{2.5}$ in Beijing: seasonal perspective, Atmos. Chem. Phys., 13, 7053–7074, doi:10.5194/acp-13-7053-2013, 2013.

Zhang, R., Li, Q., and Zhang, R.: Meteorological conditions for the persistent severe fog and haze event over eastern China in 15 January 2013, Sci. China Earth Sci., 57, 26–35, doi:10.1007/s11430-013-4774-3, 2014.

Zhang, W. C., Guo, J. P., Miao, Y. C., Liu, H., Zhang, Y., Li, Z. Q., and Zhai, P. M.: Planetary boundary layer height from CALIOP compared to radiosonde over China, Atmos. Chem. Phys., 16, 9951–9963, doi:10.5194/acp-16-9951-2016, 2016.

Zhang, X. Y., Wang, Y. Q., Niu, T., Zhang, X. C., Gong, S. L., Zhang, Y. M., and Sun, J. Y.: Atmospheric aerosol compositions in China: spatial/temporal variability, chemical signature, regional haze distribution and comparisons with global aerosols, 20 Atmos. Chem. Phys., 12, 779–799, doi:10.5194/acp-12-779-2012, 2012.

Zhang, Y. L., and Cao, F.: Fine particulate matter (PM$_{2.5}$) in China at a city level, Sci. Rep., 5, doi:10.1038/srep14884, 2015.

Zhang, Y. W., Zhang, Q., Leng, C. P., Zhang, D. Q., Cheng, T. T., Tao, J., Zhang, R. J., and He, Q. S.: Evolution of aerosol vertical distribution during particulate pollution events in Shanghai, J. Meteorol. Res., 29, 385–399, doi:10.1007/s13351-014-4089-0, 2015.

25 Zhao, H. J., Che, H. Z., Zhang, X. Y., Ma, Y. J., Wang, Y. F., Wang, H., and Wang, Y. Q.: Characteristics of visibility and particulate matter (PM) in an urban area of Northeast China, Atmos. Pollut. Res., 4, 427–434, doi:10.5094/apr.2013.049, 2013.

Zhao, X. J., Zhao, P. S., Xu, J., Meng, W., Pu, W. W., Dong, F., He, D., and Shi, Q. F.: Analysis of a winter regional haze event and its formation mechanism in the North China Plain, Atmos. Chem. Phys., 13, 5685–5696, doi:10.5194/acp-13-5685-2013, 2013.

30 Zheng, B., Zhang, Q., Zhang, Y., He, K. B., Wang, K., Zheng, G. J., Duan, F. K., Ma, Y. L., and Kimoto, T.: Heterogeneous chemistry: a mechanism missing in current models to explain secondary inorganic aerosol formation during the January 2013 haze episode in North China, Atmos. Chem. Phys., 15, 2031–2049, doi:10.5194/acp-15-2031-2015, 2015.

Zheng, G. J., Duan, F. K., Su, H., Ma, Y. L., Cheng, Y., Zheng, B., Zhang, Q., Huang, T., Kimoto, T., Chang, D., Pöschl, U., Cheng, Y. F., and He, K. B.: Exploring the severe winter haze in Beijing: the impact of synoptic weather, regional transport 35 and heterogeneous reactions, Atmos. Chem. Phys., 15, 2969–2983, doi:10.5194/acp-15-2969-2015, 2015.

已移动(插入) [4]

已移动(插入) [5]

已上移 [4]: Zhang, R., Jing, J., Tao, J., Hsu, S. C., Wang, G., Cao, J., Lee, C. S. L., Zhu, L., Chen, Z., Zhao, Y., and Shen, Z.: Chemical characterization and source apportionment of PM$_{2.5}$ in Beijing: seasonal perspective, Atmos. Chem. Phys., 13, 7053–7074, doi:10.5194/acp-13-7053-2013, 2013.
Zhang, R., Li, Q., and Zhang, R.: Meteorological conditions for the persistent severe fog and haze event over eastern China in January 2013, Sci. China Earth Sci., 57, 26–35, doi:10.1007/s11430-013-4774-3, 2014.

已上移 [5]: Zhang, W. C., Guo, J. P., Miao, Y. C., Liu, H., Zhang, Y., Li, Z. Q., and Zhai, P. M.: Planetary boundary layer height from CALIOP compared to radiosonde over China, Atmos. Chem. Phys., 16, 9951–9963, doi:10.5194/acp-16-9951-2016, 2016.

删除的内容: a

删除的内容: b

删除的内容: a

删除的内容: b

Zou, Y., Wang, Y., Zhang, Y., and Koo, J.-H.: Arctic sea ice, Eurasia snow, and extreme winter haze in China, Sci. Adv., 3, doi:10.1126/sciadv.1602751, 2017.

Table 1: The long–lasting haze and fog–haze mixed events from January 2014 to March 2015 in Beijing city

Type	Starting date / time	Ending date / time	Minimum visibility (m)	Duration (h)	Maximum $PM_{2.5}$ (µg m^{-3})	Maximum RH (%)	Weather phenomenon
Haze events	2014.01.21/ 15:00	2014.01.24/ 15:00	1364	73	264	68	–
	2014.04.11/ 22:00	2014.04.14/ 23:00	1113	74	304	89	–
	2015.02.12/ 21:00	2015.02.16/ 10:00	1667	86	263	77	–
	2015.03.04/ 22:00	2015.03.08/ 10:00	1886	83	266	72	–
Fog–haze mixed events	2014.02.19/ 21:00	2014.02.26/ 20:00	647	168/76[b]	269	92	02.26/16:00–21:25 Drizzle rain
	2014.03.22/ 22:00	2014.03.28/ 14:00	664	137/13[b]	417	94	3.28/4:30–6:20 Drizzle rain
	2014.10.06/ 22:00	2014.10.11/ 18:00	500	117/48[b]	391	100	10.08/6:40–7:50 10.08/10:30–11:50 Drizzle rain
	2014.10.16/ 21:00	2014.10.20/ 23:00	964	99/3[b]	322	100	–
	2014.10.22/ 4:00	2014.10.26/ 4:00	258	97/24[b]	379	100	–
	2014.10.28/ 23:00	2014.11.01/ 5:00	837	79/1[b]	184	100	10.29/23:00– 10.30/00:10 10.31/15:10–16:30 Drizzle rain
	2015.01.12/ 17:00	2015.01.16/ 3:00	526	83/8[b]	297	93[a]	01.14/10:00–10:20 snow

[a] the maximum RH of all valid data except missing measurement.
[b] fog–haze mixed event duration / fog duration.

Table 2: The exponential curve of visibility and PM$_{2.5}$ mass concentration for haze and fog–haze mixed events

Function	R^2	Pollutant events type
y=87.57495+12484.02388exp(–0.00787x)	0.79563	haze events
y=1043.96602+26206.87173exp(–0.01981x)	0.80668	fog–haze mixed events

x respects the mass concentration of PM$_{2.5}$ (μg m^{-3}); y respects visibility (m).

5

Table 3: Parameters of radiation from Beijing Meteorological station during the haze event

Date	20140412	20140413	20140414
Daily total radiation* (MJ m^{-2})	18.48	18.74	17.56
Daily total scattering radiation (MJ m^{-2})	10.86	11.07	12.65
Daily total horizontal plane direct radiation (MJ m^{-2})	7.62	7.67	4.91
Daily total vertical plane direct radiation (MJ m^{-2})	10.15	10.63	6.41
Daily max total radiation (W m^{-2})	835	751	715
Daily max vertical plane direct radiation (W m^{-2})	498	421	268

* Daily total radiation is the sum of daily total scattering and daily total horizontal plane direct radiation.

删除的内容: , compared with other studies

删除的内容: Function

删除的内容: k

Table 4: Parameters of radiation from Beijing Meteorological station for the fog–haze mixed event

Date	2014 1006	2014 1007	2014 1008	2014 1009	2014 1010	2014 1011
Daily total radiation* (MJ m^{-2})	17.51	12.37	9.02	8.39	9.05	8.07
Daily total scattering radiation (MJ m^{-2})	3.4	7.08	7.85	7.58	8.05	7.21
Daily total horizontal plane direct radiation (MJ m^{-2})	14.11	5.29	1.17	0.81	1	0.86
Daily total vertical plane direct radiation (MJ m^{-2})	24.94	8.28	2.23	1.82	1.84	1.4
Daily max total radiation (W m^{-2})	749	551	564	385	434	540
Daily max vertical plane direct radiation (W m^{-2})	893	366	148	91	132	202

* Daily total radiation is the sum of daily total scattering and daily total horizontal plane direct radiation.

5

Table 5 The average PM$_{2.5}$ concentration, PBL height, RH and daily radiation parameters during the haze and fog–haze mixed event

	Haze event	Fog–haze mixed event
PM$_{2.5}$ (µg m^{-3})	164.5	250.4
PBL height (m)	470	360
RH (%)	55	88
Total radiation (MJ m^{-2})	18.26	9.38
Total scattering radiation (MJ m^{-2})	11.53	7.55
Total horizontal plane direct radiation (MJ m^{-2})	6.73	1.83
Total vertical plane direct radiation (MJ m^{-2})	9.06	3.11
Max total radiation (W m^{-2})	767	398
Max vertical plane direct radiation (W m^{-2})	396	188

删除的内容: k

删除的内容: 0.47

删除的内容: 0.36
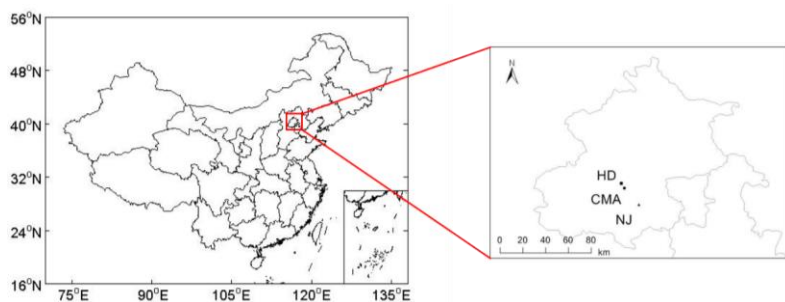
Figure 1: Geographical location of the observation sit in Beijing. CMA, HD and NJ represent China Meteorological Administration, Haidian automatic weather station and Beijing Meteorological station, respectively.

5
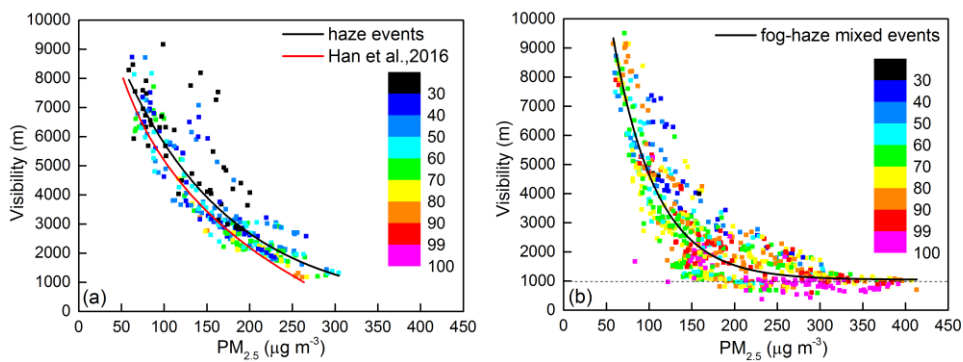
Figure 2: Relationship between the measured visibility and PM$_{2.5}$ mass concentration under different RH conditions for (a) haze and (b) fog–haze mixed events from January 2014 to March 2015 in Beijing city. The black exponential curves present the fits of the squares. The red exponential curve is the fit of daily averaged visibility and PM$_{2.5}$ concentration from October 2013 to September 2014 on stable meteorological days in Han et al. (2016)

10

删除的内容:

Figure 3: Relationship between PBL height and PM$_{2.5}$ mass concentration for (a) haze and (b) fog–haze mixed events from January 2014 to March 2015 in Beijing city

5
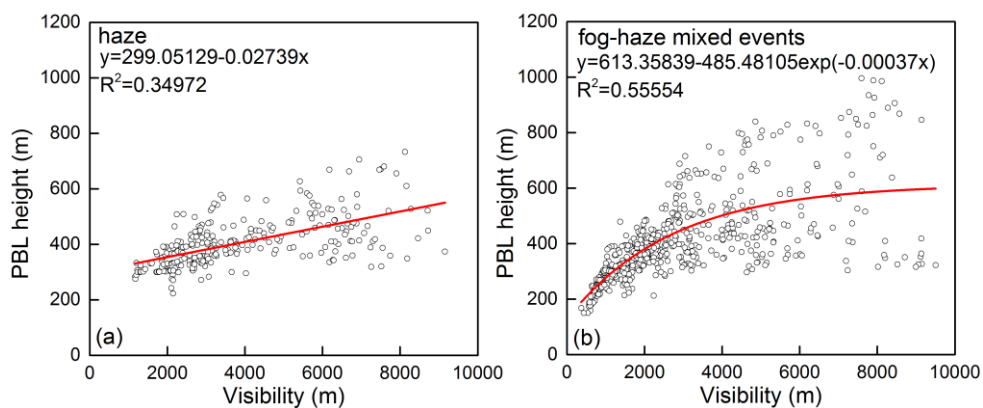
Figure 4: Relationship between visibility and PBL height for (a) haze and (b) fog-haze mixed events from January 2014 to March 2015 in Beijing city

10
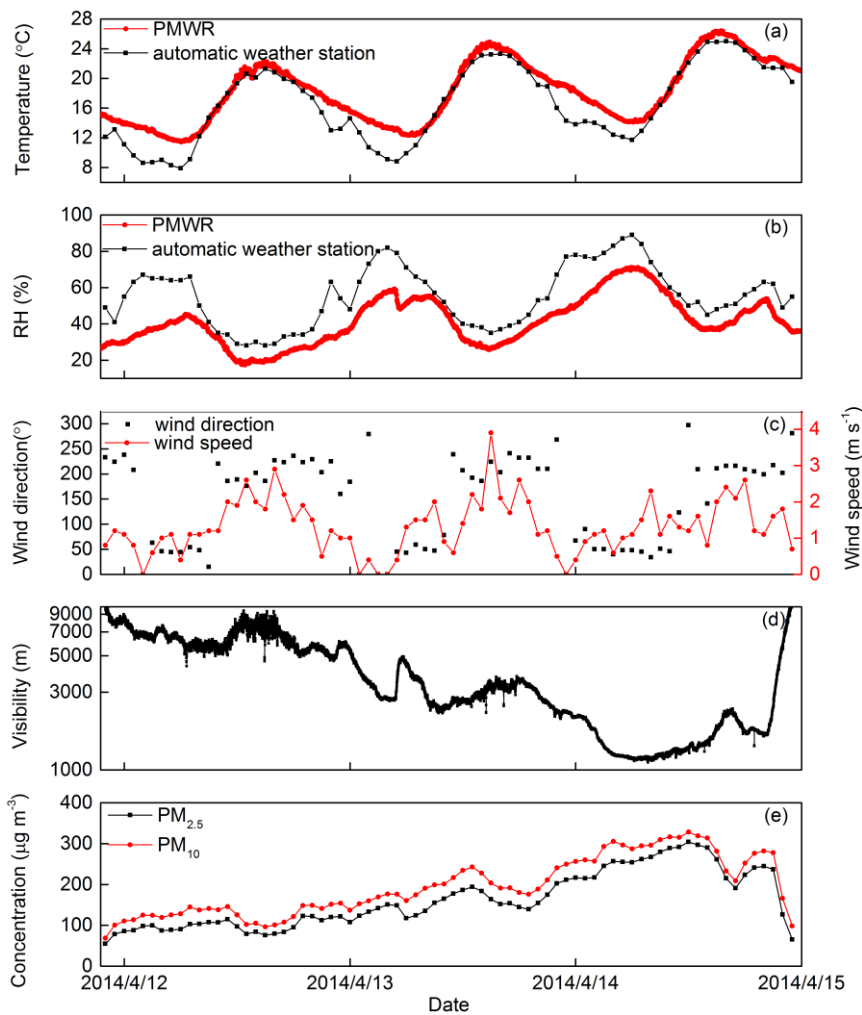
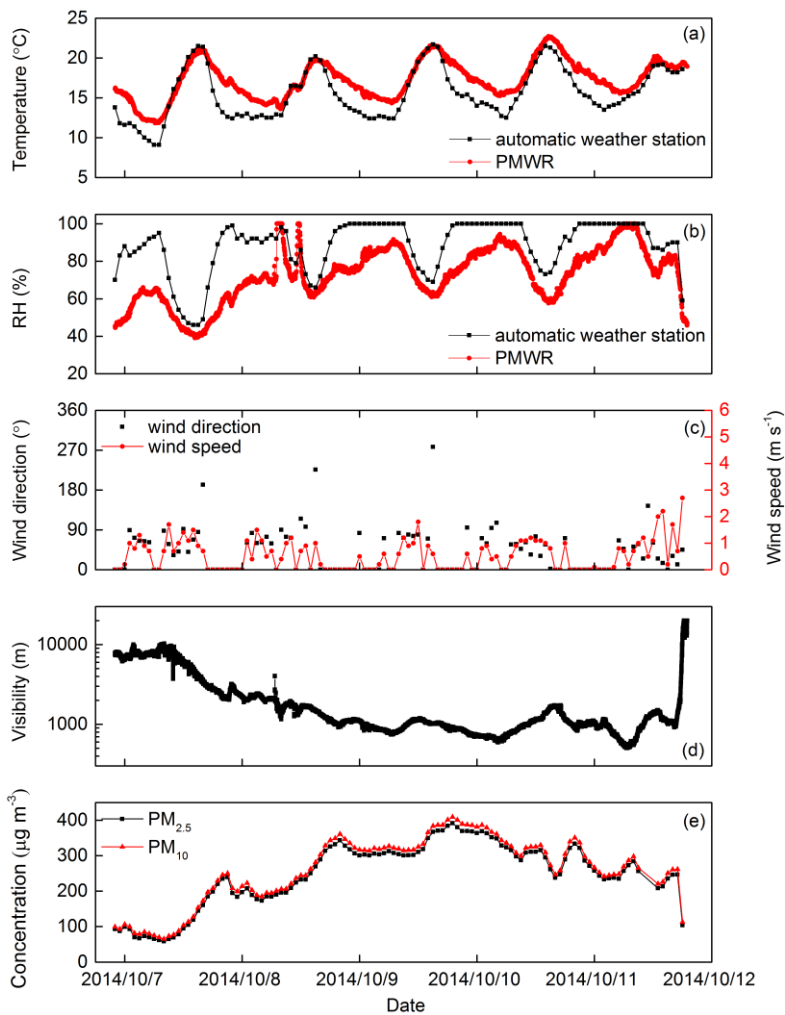**Figure 5: Temporal variations of surface meteorological and environmental parameters observed during the whole haze event in Beijing city. (a) temperature, (b) RH, (c) wind direction and wind speed, (d) visibility, (e) mass concentration of particulate matter. The temperature and RH derived from PMWR is also presented in (a) and (b).**

删除的内容: 6

5
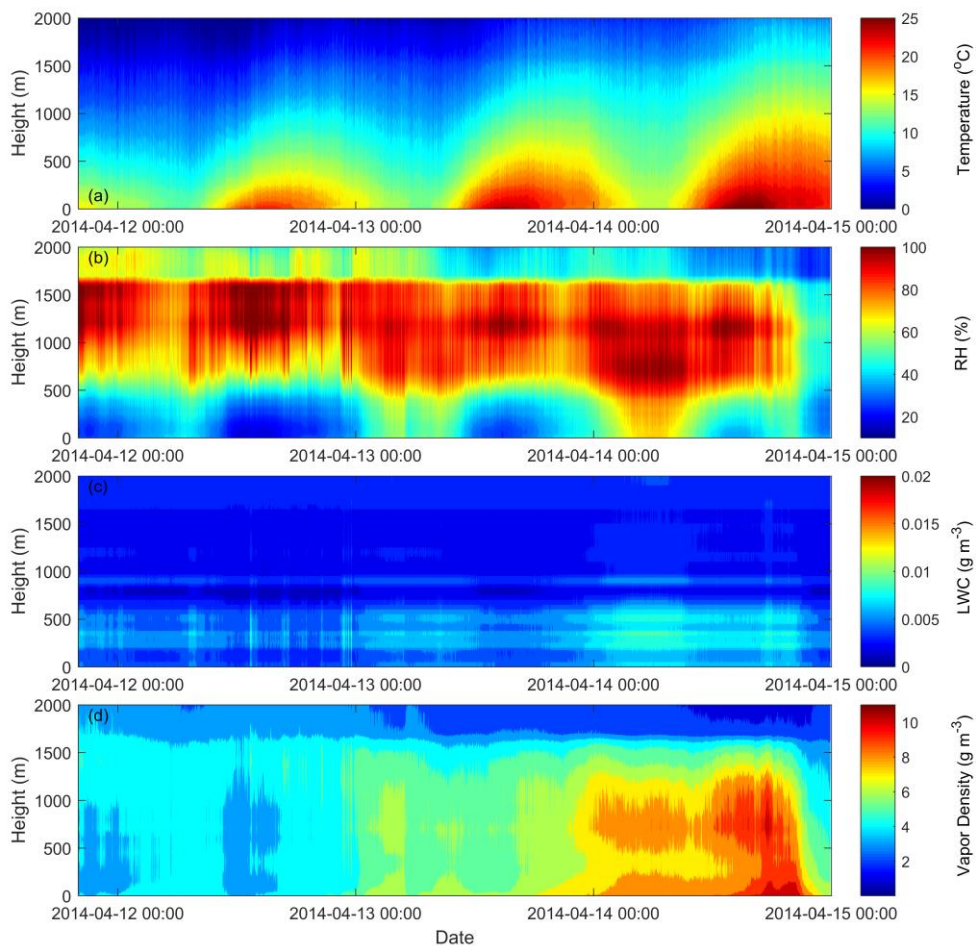
Figure 6: Time–height cross sections of (a) temperature, (b) RH, (c) LWC and (d) vapor density retrieved by MWRP during the whole haze event in Beijing city.
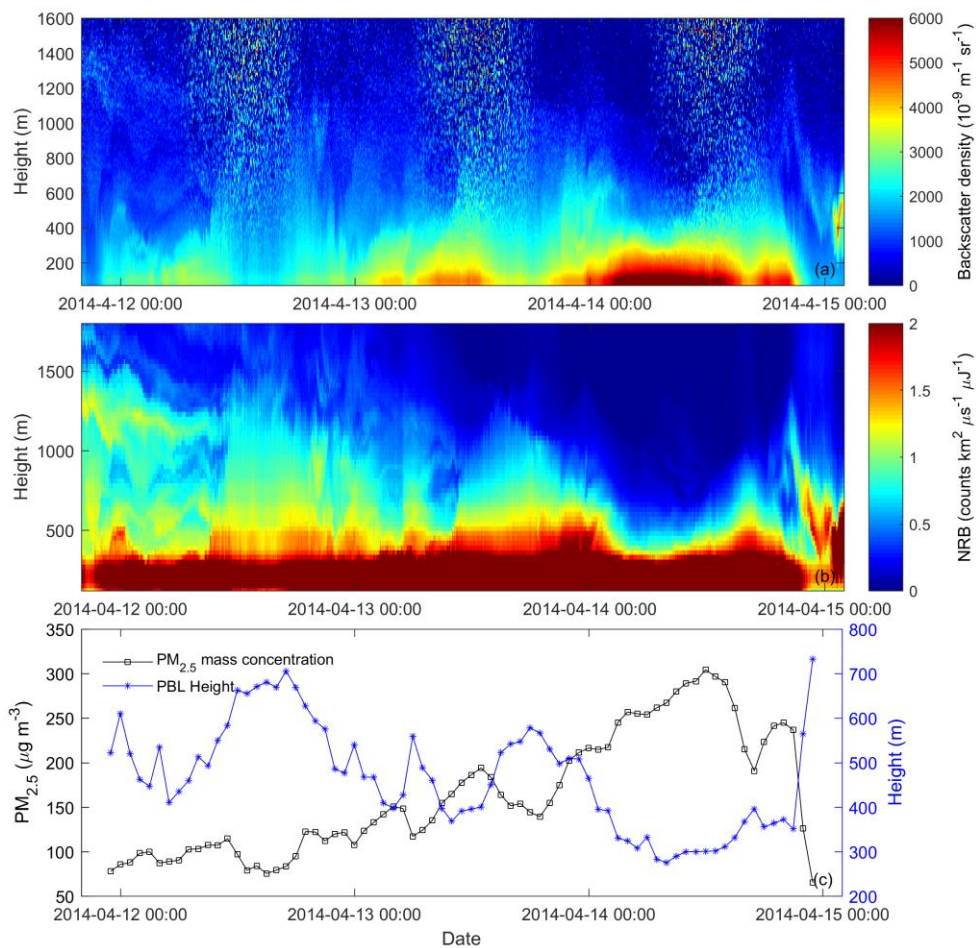
Figure 7: Time–height cross sections of (a) the backscatter density detected by the CL31 and (b) the NRB detected by the MPL, and (c) the time evolution of PM$_{2.5}$ mass concentration and PBL height retrieved by the NRB of MPL during the whole haze event in Beijing city.

5
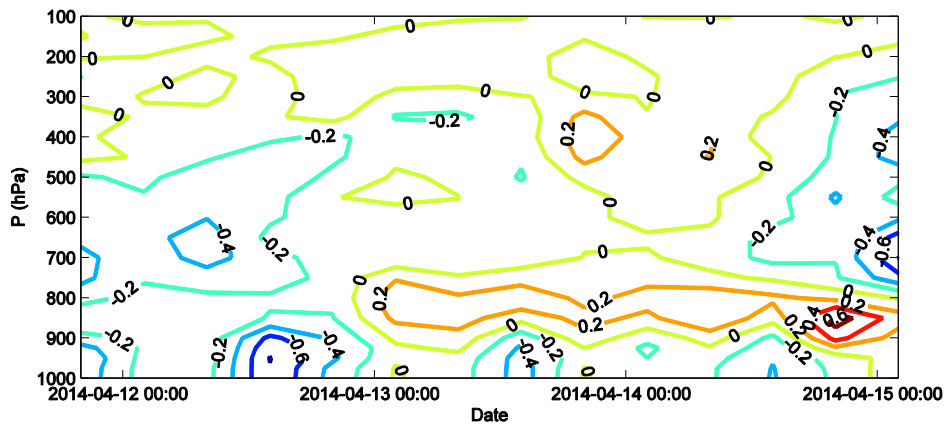
Figure 8: Time–pressure distribution of vertical velocities during the whole haze event in Beijing city. (Negative and positive numbers stand for the updrafts and downdrafts, respectively. Unit: Pa s^{-1})

Figure 2: The temperature and RH profiles during the whole haze event in Beijing city. (a) temperature and (b) RH at 8:00 LST. (c) temperature and (d) RH at 20:00 LST.

删除的内容: 10

Figure 10: Temporal variation of surface meteorological and environmental factors observed during the whole fog–haze mixed event in Beijing city. (a) temperature; (b) RH; (c) wind direction and wind speed; (d) visibility; (e) mass concentration of particulate matter. The temperature and RH derived from PMWR is also presented in (a) and (b).

删除的内容: 12

5
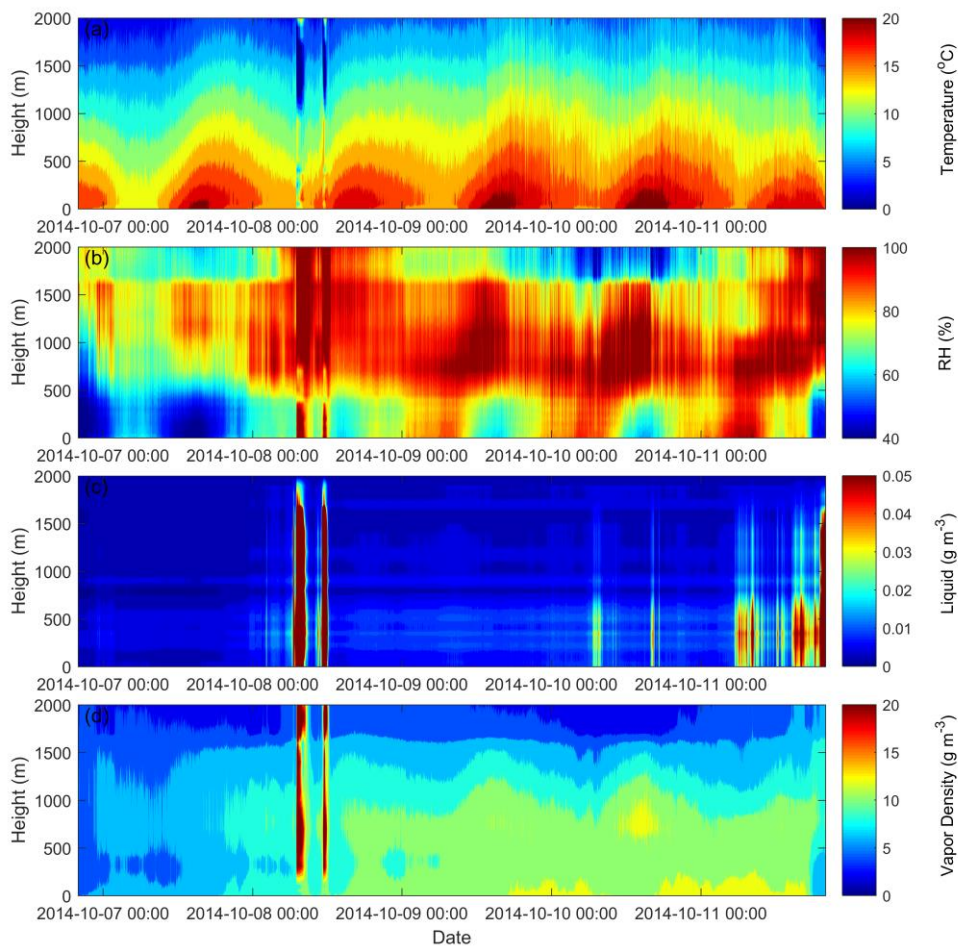
Figure 11: Time–height cross sections of (a) temperature, (b) RH, (c) LWC and (d) vapor density retrieved by MWRP during the whole fog–haze mixed event in Beijing city.
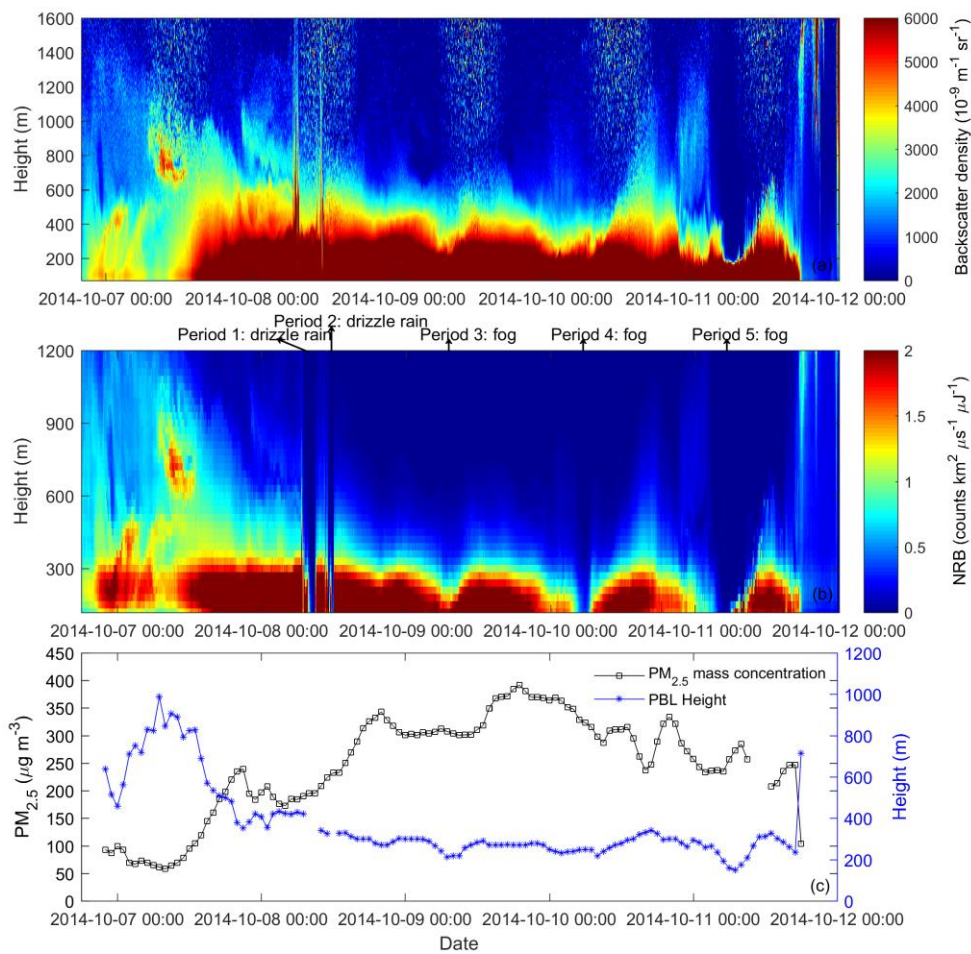
删除的内容: 3

Figure 12: Time–height cross sections of (a) the backscatter density detected by CL31 and (b) the NRB detected by MPL, and (c) the time evolution of PM$_{2.5}$ mass concentration and PBL height retrieved by the NRB of MPL during the fog–haze mixed event in Beijing city.
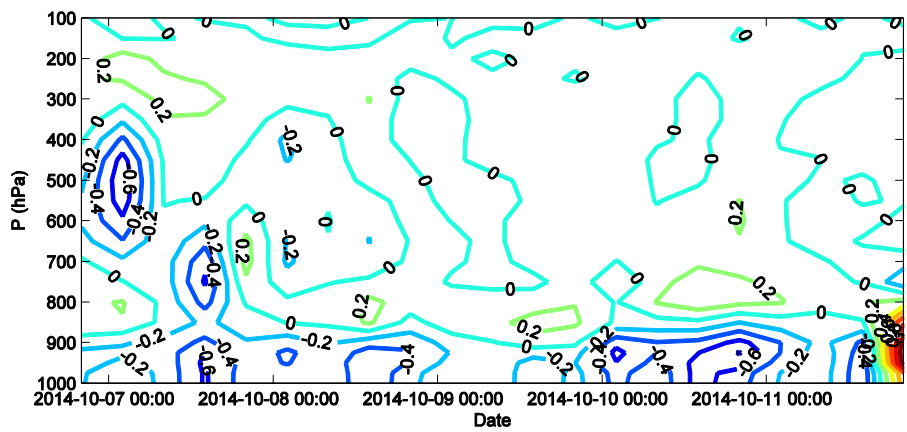
5

Figure 13: Time–pressure distribution of vertical velocities during the whole fog–haze mixed event in Beijing city. (Negative and positive numbers stand for the updrafts and downdrafts, respectively. Unit: Pa s^{-1})
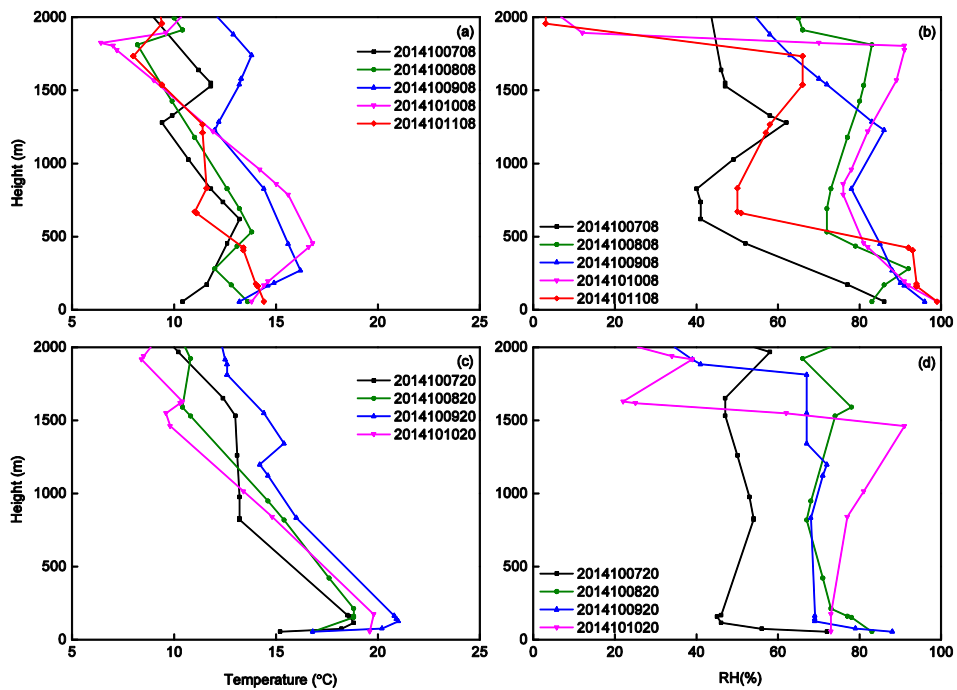
删除的内容: 5

Figure 14: The temperature and RH profiles during the whole fog–haze mixed event in Beijing city. (a) temperature and (b) RH at 8:00 LST. (c) temperature and (d) RH at 20:00 LST.

删除的内容: 6